
Chapter 11

Stability Augmentation

11.1 INTRODUCTION

In the previous chapter it is shown how the stability and control characteristics of an aeroplane may be assessed in the context of flying and handling qualities requirements. In the event that the aeroplane fails to meet the requirements in some way, then it is necessary to consider remedial action. For all except perhaps the most trivial of problems it is not usually practical to modify the aerodynamic design of the aeroplane once its design has been finalised. Quite often the deficiencies occur simply as a result of the requirement for the aeroplane to operate over an extended flight envelope and not necessarily as a result of an aerodynamic design oversight. Alternatively, this might be explained as the effects of aerodynamic non-linearity. The preferred solution is, therefore, to artificially modify, or *augment*, the apparent stability characteristics of the airframe. This is most conveniently achieved by the introduction of *negative feedback* in which the output signals from motion sensors are processed in some way and used to drive the appropriate control surfaces via actuators. The resultant *closed loop control system* is similar in many respects to the classical servo mechanism familiar to the control engineer. A significant advantage of this approach is that the analysis of the augmented, or closed loop, aircraft makes full use of the well-established tools of the control engineer. The *systems* approach to flight dynamics analysis has already been introduced in earlier chapters where, for example, control engineering tools have been utilised for solving the equations of motion.

A functional block diagram of a typical *flight control system* (FCS) is shown in Fig. 11.1. It is assumed that the primary flying controls are mechanical such that pilot commands drive the control surfaces via control actuators which augment the available power to levels sufficient to overcome the aerodynamic loads on the surfaces. The *electronic flight control system* (EFCS) comprises two feedback loops both of which derive their control signals from motion sensors appropriate to the requirements of the *control laws*. The outputs from the inner and outer loop controllers are electronically summed and the resultant signal controls the aircraft via a small servo actuator. Typically, the servo actuator is an electro-hydraulic device which converts low power electrical signals to mechanical signals at a power level compatible with those originating at the pilot to which it is mechanically summed. Although only a single control axis is indicated in Fig. 11.1, it is important to appreciate that the FCS will, in general, include closed loop controllers operating on the roll, pitch and yaw control axes of the aircraft simultaneously and may even extend to include closed loop engine control as well. Thus multi-variable feedback involving many separate control loops is implied, which is typical of many modern FCS.

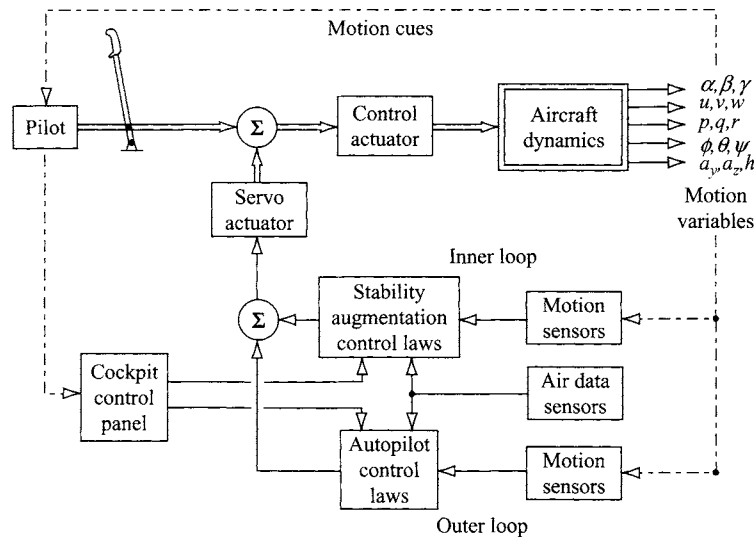


Figure 11.1 A typical flight control system.

The *inner loop* provides stability augmentation and is usually regarded as essential for continued proper operation of the aircraft. The inner loop control system alone comprises the *stability augmentation system* (SAS), it is usually the first part of the FCS to be designed and together with the airframe comprises the *augmented aircraft*.

The *outer loop* provides the *autopilot* which, as its name suggests, enables the pilot to fly various manoeuvres under automatic control. Although necessary for operational reasons, an autopilot is not essential for the provision of a safe well behaved aircraft. The *autopilot control modes* are designed to function with the augmented aircraft and may be selectively engaged as required to automate the piloting task. Their use is intended to release the pilot from the monotony of flying steady conditions manually and to fly precision manoeuvres in adverse conditions which may be at, or beyond, the limits of human capability. Autopilot control modes vary from the very simple, for example *height hold*, to the very complex, for example *automatic landing*.

Since, typically, for most aircraft the *control law gains* required to effect good stability, control and handling vary with operating condition, it is necessary to make provision for their continuous adjustment. The variations often arise as a result of variations in the aerodynamic properties of the airframe over the flight envelope. For example, at low speed the aerodynamic effectiveness of the control surfaces is generally less than at high speed. This means that higher *control gains* are required at low speeds and *vice versa*. It is, therefore, common practice to vary, or *schedule*, gains as a function of flight condition. Commonly used flight condition variables are dynamic pressure, Mach number, altitude and so on, information which is grouped under the description of *air data*. Generally, air data information would be available to all control laws in a FCS as indicated in Fig. 11.1.

A control panel is provided in the cockpit to enable the pilot to control and monitor the operation of the FCS. SAS controls are usually minimal and enable the pilot to monitor the system for correct, and hence safe, operation. In some cases he may also be

provided with means for selectively isolating parts of the SAS. On the other hand, the autopilot control panel is rather more substantial. Controls are provided to enable the pilot to set up, engage and disengage the various autopilot mode functions. The control panel also enables him to monitor progress during the automated manoeuvre selected.

In piloted phases of flight the autopilot would normally be disengaged and, as indicated in Fig. 11.1 the pilot would derive his perception of flying and handling qualities from the motion cues provided by the augmented aircraft. Thus the inner loop control system provides the means by which all aspects of stability, control and handling may be tailored in order to improve the characteristics of the basic aircraft.

11.1.1 The control law

The control law is a mathematical expression which describes the function implemented by an augmentation or autopilot controller. For example, a very simple and very commonly used control law describing an inner loop control system for augmenting yaw damping is

$$\zeta(s) = K_\zeta \delta_\zeta(s) - K_r \left(\frac{s}{1 + sT} \right) r(s) \quad (11.1)$$

Equation (11.1) simply states that the control signal applied to the rudder $\zeta(s)$ comprises the sum of the pilot command $\delta_\zeta(s)$ and yaw rate feedback $r(s)$. The gain K_ζ is the mechanical gearing between rudder pedals and rudder and the gain K_r is the all important feedback gain chosen by design to optimise the damping in yaw. The second term in equation (11.1) is negative since negative feedback is required to increase stability in yaw. The second term also, typically, includes a *washout*, or *high-pass*, filter with a time constant of around 1 or 2 s. The filter is included to block yaw rate feedback in steady turning flight in order to prevent the feedback loop opposing the pilot command once the rudder pedals are returned to centre after manoeuvre initiation. However, the filter is effectively *transparent* during transient motion thereby enabling the full effect of the feedback loop to quickly damp out the yaw oscillation.

11.1.2 Safety

In any aeroplane fitted with a FCS safety is the most critical issue. Since the FCS has direct “access” to the control surfaces considerable care must be exercised in the design of the system to ensure that under no circumstances can a maximum instantaneous uncontrolled command be applied to any control surface. For example, a sensor failure might cause its output to *saturate* at its maximum possible value. This signal, in turn, is *conditioned* by the control law to apply what could well be a demand of magnitude sufficient to cause a maximum control surface displacement. The resulting *failure transient* might well be some kind of hazardous divergent response. Clearly, steps must be taken in the design of the FCS architecture to incorporate mechanisms to protect the aircraft from partial or total system malfunction.

The design of *safety critical* FCS architectures, as opposed to the simpler problem of control law design, is a substantial subject in its own right. However, at an introductory

level, it is sufficient to appreciate that the requirements for safety can sometimes override the requirements for control, especially when relatively large control system gains are necessary. For simple SAS of the kind exemplified by the control law, equation (11.1), the problem may be overcome by limiting the maximum values of the control signals, giving rise to what is referred to as a *limited authority* control system. In more complex FCS where authority limiting is not acceptable for control reasons, it may be necessary to employ control system *redundancy*. Redundant FCS comprise two, or more, systems which are functionally similar and which normally operate in parallel. In the event of a system malfunction, the faulty equipment is isolated leaving the remaining *healthy* system components to continue the augmentation task. In such systems, automatic fault containment can reduce the failure transient to an imperceptible level. It is then necessary to provide the pilot with information enabling him to continuously *monitor* the state of health of the FCS on an appropriate cockpit display.

11.1.3 SAS architecture

The architecture of an inner loop SAS is shown in Fig. 11.2. This classical system description assumes an aeroplane with mechanical flying controls to which the EFCS connects via the servo actuator. The system is typical of those applied to many aeroplanes of the 1950s and 1960s. For the purpose of discussion one control axis only is shown in Fig. 11.2 but it applies equally well to the remaining axes.

As above, the essential element of the SAS is the control law, the remaining components of the system are the necessary by-products of its implementation. Noise filtering is often required to remove unwanted information from sensor outputs. At best noise can cause unnecessary actuator activity and, at worst, may even give rise to unwanted aircraft motion. Sometimes, when the sensor is located in a region of significant structural flexibility the “noise” may be due to normal structure distortion, the control demand may then exacerbate the structure bending to result in structural divergence. Thus an unwanted unstable structural feedback loop can be inadvertently

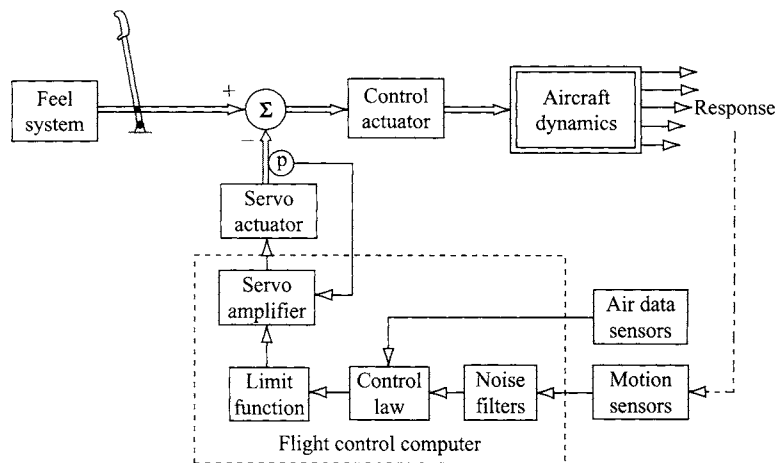


Figure 11.2 A typical SAS.

created. The cure usually involves narrow band filtering to remove information from the sensor output signal at sensitive structural bending mode frequencies.

The fundamental role of the SAS is to minimise response transients following an upset from equilibrium. Therefore, when the system is working correctly in non-maneuvring flight the response variables will have values at, or near, zero since the action of the negative feedback loop is to drive the *error* to zero. Thus a SAS does not normally require large authority control and the limit function would typically limit the amplitude of the control demand to, say, $\pm 10\%$ of the total surface deflection. The limiter may also incorporate a rate limit function to further contain transient response by imposing a maximum actuator slew rate demand. It is important to realise that whenever the control demand exceeds the limit the system saturates, becomes temporarily open loop and the dynamics of the aircraft revert to those of the unaugmented airframe. This is not usually considered to be a problem as saturation is most likely to occur during manoeuvring flight when the pilot has very “tight” manual control of the aeroplane and effectively replaces the SAS control function.

The servo amplifier together with the servo actuator provide the interface between the FCS and the mechanical flying controls. These two elements comprise a classical position servo mechanism as indicated by the electrical feedback from a position sensor on the servo actuator output. Mechanical amplitude limiting may well be applied to the servo actuator as well as, or instead of, the electronic limits programmed into the flight control computer.

Since the main power control actuator, also a classical mechanical servo mechanism, breaks the direct mechanical link between the pilots controller and the control surface, the control feel may bear little resemblance to the aerodynamic surface loads. The feedback loop around the control actuator would normally be mechanical since it may well need to function with the SAS inoperative. It is therefore necessary to augment the controller feel characteristics as well. The feel system may be a simple non-linear spring but, is more commonly an electro-hydraulic device, often referred to as a *Q-feel system* since its characteristics are scheduled with dynamic pressure Q . Careful design of the feel system enables the apparent controls free manoeuvre margin of the aircraft to be adjusted independently of the other inter-related stability parameters.

When the mechanical flying controls are dispensed with altogether and replaced by an electrical or electronic link the resultant SAS is described as a fly-by-wire (FBW) system. When the FCS shown in Fig. 11.2 is implemented as a FBW system its functional structure is changed to that shown in Fig. 11.3. The SAS inner control loop remains unchanged, the only changes relate to the primary control path and the actuation systems.

Since the only mechanical elements in the FCS are the links between the control actuator and the surfaces it is usual for the servo actuator and the control actuator to be combined into one unit. Its input is then the electrical control demand from the flight control computer and its output is the control surface deflection. An advantage of an integrated actuation system is the facility for mechanical simplification since the feedback loops may be closed electrically rather than by a combination of electrical and mechanical feedbacks. Mechanical feedback is an unnecessary complication since in the event of a flight control computer failure the aeroplane would be uncontrollable. Clearly, this puts a rather more demanding emphasis on the safety of the FCS.

Primary control originates at the pilots control inceptors which, since they are not constrained by mechanical control linkages, may now take alternative forms,

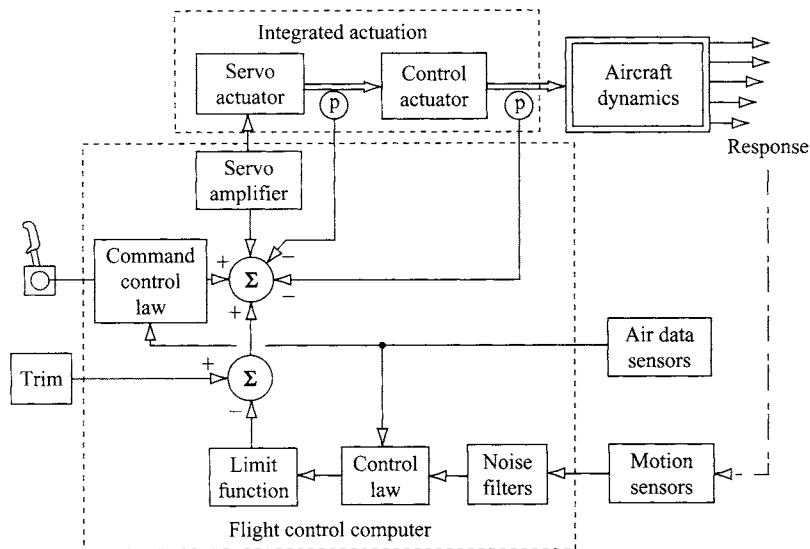


Figure 11.3 A typical FBW command and stability augmentation system.

for example, a *side-stick controller*. The control command signal is conditioned by a command control law which determines the control and response characteristics of the augmented aircraft. Since the command control law is effectively *shaping* the command signal in order to achieve acceptable response characteristics, its design is a means for augmenting handling qualities independently of stability augmentation. For this reason, a FCS with the addition of command path augmentation is known as a command and stability augmentation system (CSAS).

Provision is shown in Fig. 11.3 for an electrical trim function since not all aircraft with advanced technology FCS employ mechanical trimmers. The role of the trim function is to set the datum control signal value, and hence the control surface angle, to that required to maintain the chosen equilibrium flight condition. The precise trim function utilised would be application dependent and in some cases an entirely automatic trim system might be implemented. In this latter case no pilot trimming facility is required.

Since the pilot must have full authority control over the aircraft at all times it is implied that the actuation system must also have full authority control. The implications for safety following a failure in any component in the primary control path is obviously critical. As for the simple SAS the feedback control signal may be authority limited prior to summing with the primary control commands and this will protect the system against failures within the stability augmentation function. However, this solution cannot be used in the primary control path. Consequently, FBW systems must have reliability of a very high order and this usually means significant levels of redundancy in the control system architecture together with sophisticated mechanisms for identifying and containing the worst effects of system malfunction.

In the above brief description of a FBW system it is assumed that all control signals are electrical and transmitted by normal electrical cables. However, since most modern flight control computers are digital the transmission of control signals

also involves digital technology. Digital signals can also be transmitted optically with some advantage, especially in the demanding environment within aircraft. Today it is common for optical signal transmission to be used in FCS if for no other reason than to maintain electrical isolation between redundant components within the system. There is no reason why optical signalling should not be used for primary flight control and there are a small number of systems currently flying which are optically signalled. Such a control system is referred to as a fly-by-light (FBL) system and the control function is essentially the same as that of the FBW system or simple SAS it replaces. In fact, it is most important to recognise that for a given aeroplane the stability augmentation function required of the FCS is the same irrespective of the architecture adopted for its implementation. In the context of stability augmentation there is nothing special or different in a FBW or FBL system solution.

11.1.4 Scope

In the preceding paragraphs an attempt has been made to introduce and review some of the important issues concerning FCS design in general. In particular, the role of the SAS or CSAS and the possible limitation of the control function imposed by the broader concerns of system structure has been emphasised. The temptation now is to embark on a discussion of FCS design but, unfortunately, such a vast subject is beyond the scope of the present book.

Rather, the remainder of this chapter is concerned with the very fundamental, and sometimes subtle, way in which feedback may be used to augment the dynamics of the basic aircraft. It is very important that the flight dynamicist understands the way in which his chosen control system design augments the stability and control properties of the airframe. It is not good enough to treat the aircraft like an arbitrary *plant* and to design a *controller* to meet a predefined set of performance requirements, an approach much favoured by control system designers. It is vital that the FCS designer retains a complete understanding of the implications of his design decisions throughout the design process. In the interests of *functional visibility*, and hence of safety, it is important that FCS are made as simple as possible. This is often only achievable when the designer has a complete and intimate understanding of the design process.

11.2 AUGMENTATION SYSTEM DESIGN

The most critical aspect of FCS design is concerned with the design of the inner loop control law. The design objective being to endow the aircraft with good stability, control and handling characteristics throughout its flight envelope. Today, a FBW system gives the designer the greatest freedom of choice as to how he might allocate the control law functions for “optimum” performance. The main CSAS control functions are indicated in the rather over simplified representation shown in Fig. 11.4. The problem confronting the FCS designer is to design suitable functions for the command, feed forward and feedback paths of the CSAS and obviously, it is necessary to appreciate the role of each path in the overall context of aircraft stability augmentation.

The *feedback path* comprises the classical inner loop SAS whose primary role is to augment static and dynamic stability. It generally improves flying and handling

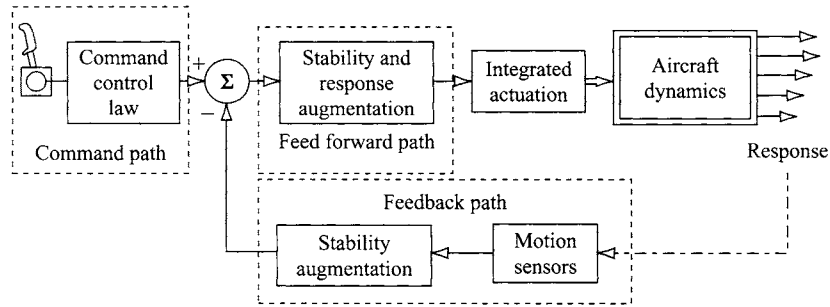


Figure 11.4 Inner loop control functions.

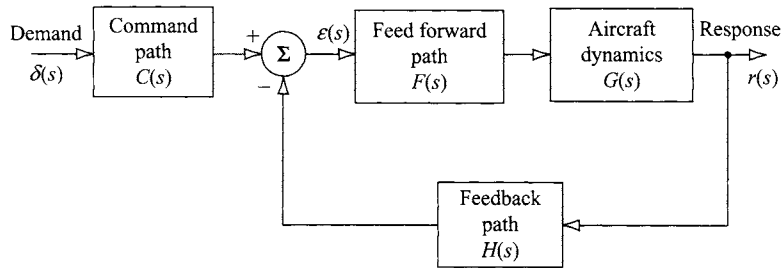


Figure 11.5 Inner loop transfer function representation.

qualities but may not necessarily lead to ideal handling qualities since it has insufficient direct control over *response shaping*.

The *feed forward path* is also within the closed loop and its function augments stability in exactly the same way as the feedback path. However, it has a direct influence on command signals as well and by careful design its function may also be used to exercise some degree of response shaping. Its use in this role is limited since the stability augmentation function must take priority.

The *command path* control function provides the principal means for response shaping, it has no influence on stability since it is outside the closed loop. This assumes, of course, that the augmented aircraft may be represented as a *linear* system. The command path indicated in Fig. 11.4 assumes entirely electronic signalling as appropriate to a FBW system. However, there is no reason why the command and feed forward paths should not comprise a combination of parallel electrical and mechanical paths, an architecture commonly employed in aircraft of the 1960s and 1970s. In such systems it is only really practical to incorporate all, other than very simple, signal shaping into the electrical signal paths.

Further analysis of the simple CSAS structure may be made if it is represented by its transfer function equivalent as shown in Fig. 11.5.

With reference to Fig. 11.5 the *control error* signal $\varepsilon(s)$ is given by

$$\varepsilon(s) = C(s)\delta(s) - H(s)r(s) \quad (11.2)$$

where, $\delta(s)$ and $r(s)$ are the command and response signals respectively and, $C(s)$ and $H(s)$ are the command path and feedback path transfer functions respectively. The output response $r(s)$ is given by

$$r(s) = F(s)G(s)\varepsilon(s) \quad (11.3)$$

where, $F(s)$ is the feed forward path transfer function and $G(s)$ is the all important transfer function representing the basic airframe. Combining equations (11.2) and (11.3) to eliminate the error signal, the closed loop transfer function is obtained

$$\frac{r(s)}{\delta(s)} = C(s) \left(\frac{F(s)G(s)}{1 + F(s)G(s)H(s)} \right) \quad (11.4)$$

Thus the transfer function given by equation (11.4) is that of the augmented aircraft and replaces that of the unaugmented aircraft $G(s)$. Clearly, by appropriate choice of $C(s)$, $F(s)$ and $H(s)$ the FCS designer has considerable scope for tailoring the stability, control and handling characteristics of the augmented aircraft. The characteristic equation of the augmented aircraft is given by

$$\Delta(s)_{aug} = 1 + F(s)G(s)H(s) = 0 \quad (11.5)$$

Note that the command path transfer function $C(s)$ does not appear in the characteristic equation therefore, as noted above, it cannot influence stability in any way.

Let the aircraft transfer function be denoted by its numerator and denominator in the usual way,

$$G(s) = \frac{N(s)}{\Delta(s)} \quad (11.6)$$

Let the feed forward transfer function be a simple proportional gain

$$F(s) = K \quad (11.7)$$

and let the feedback transfer function be represented by a typical lead-lag function,

$$H(s) = \left(\frac{1 + sT_1}{1 + sT_2} \right) \quad (11.8)$$

Then the transfer function of the augmented aircraft, equation (11.4), may be written,

$$\frac{r(s)}{\delta(s)} = C(s) \left(\frac{KN(s)(1 + sT_2)}{\Delta(s)(1 + sT_2) + KN(s)(1 + sT_1)} \right) \quad (11.9)$$

Now let the roles of $F(s)$ and $H(s)$ be reversed, whence,

$$F(s) = \left(\frac{1 + sT_1}{1 + sT_2} \right) \quad H(s) = K \quad (11.10)$$

In this case the transfer function of the augmented aircraft, equation (11.4), may be written

$$\frac{r(s)}{\delta(s)} = C(s) \left(\frac{KN(s)(1 + sT_1)}{\Delta(s)(1 + sT_2) + KN(s)(1 + sT_1)} \right) \quad (11.11)$$

Comparing the closed loop transfer functions, equations (11.9) and (11.11), it is clear that the stability of the augmented aircraft is unchanged since the denominators are the same. However, the numerators are different implying a difference in the response to control and this difference can be exploited to some advantage in some FCS applications.

Now if the gains in the control system transfer functions $F(s)$ and $H(s)$ are deliberately made large such that at all frequencies over the bandwidth of the aeroplane

$$F(s)G(s)H(s) \gg 1 \quad (11.12)$$

then, the closed loop transfer function, equation (11.4), is given approximately by

$$\frac{r(s)}{\delta(s)} \approx \frac{C(s)}{H(s)} \quad (11.13)$$

This demonstrates the important result that in highly augmented aircraft the stability and control characteristics may become substantially independent of the dynamics of the basic airframe. In other words, the stability, control and handling characteristics are largely determined by the design of the CSAS, in particular the design of the transfer functions $C(s)$ and $H(s)$. In practice, this situation is only likely to be encountered when the basic airframe is significantly unstable. This illustration implies that augmentation would be provided by a FBW system and ignores the often intrusive effects of the dynamics of the FCS components.

11.3 CLOSED LOOP SYSTEM ANALYSIS

For the purpose of illustrating how motion feedback augments basic airframe stability consider the very simple example in which pitch attitude is fed back to elevator. The most basic essential features of the control system are shown in Fig. 11.6. In this example the controller comprises a simple gain constant K_θ in the feedback path.

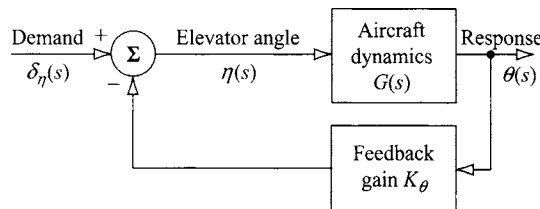


Figure 11.6 A simple pitch attitude feedback system.

The control law is given by

$$\eta(t) = \delta_\eta(t) - K_\theta \theta(t) \quad (11.14)$$

and the appropriate aircraft transfer function is

$$\frac{\theta(s)}{\eta(s)} = G(s) = \frac{N_\eta^\theta(s)}{\Delta(s)} \quad (11.15)$$

Therefore, the closed loop transfer function of the augmented aircraft is

$$\frac{\theta(s)}{\delta_\eta(s)} = \frac{N_\eta^\theta(s)}{\Delta(s) + K_\theta N_\eta^\theta(s)} \quad (11.16)$$

and the augmented characteristic equation is

$$\Delta(s)_{aug} = \Delta(s) + K_\theta N_\eta^\theta(s) = 0 \quad (11.17)$$

Thus, for a given aircraft transfer function its stability may be augmented by selecting a suitable value of feedback gain K_θ . Clearly when K_θ is zero there is no feedback, the aircraft is said to be *open loop* and its stability characteristics are un-modified. As the value of K_θ is increased so the degree of augmentation is increased and the stability modes increasingly diverge from those of the open loop aircraft. Note that the open and closed loop transfer function numerators, equations (11.15) and (11.16), are the same in accordance with the findings of Section 11.2.

Alternatively, the closed loop equations of motion may be obtained by incorporating the control law into the open loop equations of motion. The open loop equations of motion in state space form and referred to a body axis system are given by equation (4.67),

$$\begin{bmatrix} \dot{u} \\ \dot{w} \\ \dot{q} \\ \dot{\theta} \end{bmatrix} = \begin{bmatrix} x_u & x_w & x_q & x_\theta \\ z_u & z_w & z_q & z_\theta \\ m_u & m_w & m_q & m_\theta \\ 0 & 0 & 1 & 0 \end{bmatrix} \begin{bmatrix} u \\ w \\ q \\ \theta \end{bmatrix} + \begin{bmatrix} x_\eta & x_\tau \\ z_\eta & z_\tau \\ m_\eta & m_\tau \\ 0 & 0 \end{bmatrix} \begin{bmatrix} \eta \\ \tau \end{bmatrix} \quad (11.18)$$

substitute the control law expression for η , equation (11.14), into equation (11.18) and rearrange to obtain the closed loop state equation,

$$\begin{bmatrix} \dot{u} \\ \dot{w} \\ \dot{q} \\ \dot{\theta} \end{bmatrix} = \begin{bmatrix} x_u & x_w & x_q & x_\theta - K_\theta x_\eta \\ z_u & z_w & z_q & z_\theta - K_\theta z_\eta \\ m_u & m_w & m_q & m_\theta - K_\theta m_\eta \\ 0 & 0 & 1 & 0 \end{bmatrix} \begin{bmatrix} u \\ w \\ q \\ \theta \end{bmatrix} + \begin{bmatrix} x_\eta & x_\tau \\ z_\eta & z_\tau \\ m_\eta & m_\tau \\ 0 & 0 \end{bmatrix} \begin{bmatrix} \delta_\eta \\ \tau \end{bmatrix} \quad (11.19)$$

Clearly, the effect of θ feedback is to modify, or augment the derivatives x_θ , z_θ and m_θ . For a given value of the feedback gain K_θ equation (11.19) may be solved in the usual way to obtain all of the closed loop longitudinal response transfer functions,

$$\frac{u(s)}{\delta_\eta(s)} = \frac{N_\eta^u(s)}{\Delta(s)_{aug}} \quad \frac{w(s)}{\delta_\eta(s)} = \frac{N_\eta^w(s)}{\Delta(s)_{aug}} \quad \frac{q(s)}{\delta_\eta(s)} = \frac{N_\eta^q(s)}{\Delta(s)_{aug}} \quad \frac{\theta(s)}{\delta_\eta(s)} = \frac{N_\eta^\theta(s)}{\Delta(s)_{aug}}$$

and

$$\frac{u(s)}{\tau(s)} = \frac{N_\tau^u(s)}{\Delta(s)_{aug}} \quad \frac{w(s)}{\tau(s)} = \frac{N_\tau^w(s)}{\Delta(s)_{aug}} \quad \frac{q(s)}{\tau(s)} = \frac{N_\tau^q(s)}{\Delta(s)_{aug}} \quad \frac{\theta(s)}{\tau(s)} = \frac{N_\tau^\theta(s)}{\Delta(s)_{aug}}$$

where, $\Delta(s)_{aug}$ is given by equation (11.17).

An obvious problem with this analytical approach is the need to solve equation (11.19) repetitively for a range of values of K_θ in order to determine the value which gives the desired stability characteristics. Fortunately, the *root locus plot* provides an extremely effective graphical tool for the determination of feedback gain without the need for repetitive computation.

Example 11.1

The pitch attitude response to elevator transfer function for the Lockheed F-104 Starfighter in a take-off configuration was obtained from Teper (1969) and may be written in factorised form,

$$\frac{\theta(s)}{\eta(s)} = \frac{-4.66(s + 0.133)(s + 0.269)}{(s^2 + 0.015s + 0.021)(s^2 + 0.911s + 4.884)} \quad (11.20)$$

Inspection of the denominator of equation (11.20) enables the stability mode characteristics to be written down

$$\text{Phugoid damping ratio } \zeta_p = 0.0532$$

$$\text{Phugoid undamped natural frequency } \omega_p = 0.145 \text{ rad/s}$$

$$\text{Short period damping ratio } \zeta_s = 0.206$$

$$\text{Short period undamped natural frequency } \omega_s = 2.21 \text{ rad/s}$$

The values of these characteristics suggests that the short period mode damping ratio is unacceptably low, the remainder being acceptable. Therefore, stability augmentation is required to increase the short period damping ratio.

In the first instance, assume a SAS in which pitch attitude is fed back to elevator through a constant gain K_θ in the feedback path. The SAS is then exactly the same as that shown in Fig. 11.6 and as before, the control law is given by equation (11.14). However, since the aircraft transfer function, equation (11.20), is negative a negative feedback loop effectively results in overall positive feedback which is, of course, destabilising. This situation arises frequently in aircraft control and, whenever a negative open loop transfer function is encountered it is necessary to assume a positive feedback loop, or equivalently a negative value of the feedback gain, in order to obtain a stabilising control system. *Care must always be exercised in this context.* Therefore, in this particular example, when the negative sign of the open loop transfer function is taken into account the closed loop transfer function, equation (11.16), of the augmented aircraft may be written,

$$\frac{\theta(s)}{\delta_\eta(s)} = \frac{N_\eta^\theta(s)}{\Delta(s) - K_\theta N_\eta^\theta(s)} \quad (11.21)$$

Substitute the open loop numerator and denominator polynomials from equation (11.20) into equation (11.21) and rearrange to obtain the closed loop transfer function

$$\frac{\theta(s)}{\delta_\eta(s)} = \frac{-4.66(s + 0.133)(s + 0.269)}{s^4 + 0.926s^3 + (4.919 + 4.66K_\theta)s^2 + (0.095 + 1.873K_\theta)s + (0.103 + 0.167K_\theta)} \quad (11.22)$$

Thus, the augmented characteristic equation is

$$\Delta(s)_{aug} = s^4 + 0.927s^3 + (4.919 + 4.66K_\theta)s^2 + (0.095 + 1.873K_\theta)s + (0.103 + 0.167K_\theta) = 0 \quad (11.23)$$

The effect of the feedback gain K_θ on the longitudinal stability modes of the F-104 can only be established by repeatedly solving equation (11.23) for a range of suitable gain values. However, a reasonable appreciation of the effect of K_θ on the stability modes can be obtained from the approximate solution of equation (11.23). Writing equation (11.23),

$$As^4 + Bs^3 + Cs^2 + Ds + E = 0 \quad (11.24)$$

then an approximate solution is given by equation (6.13).

Thus the characteristics of the short period mode are given approximately by

$$s^2 + \frac{B}{A}s + \frac{C}{A} = s^2 + 0.927s + (4.919 + 4.66K_\theta) = 0 \quad (11.25)$$

Whence,

$$\begin{aligned} \omega_s &= \sqrt{(4.919 + 4.66K_\theta)} \\ 2\zeta_s\omega_s &= 0.927 \text{ rad/s} \end{aligned} \quad (11.26)$$

It is therefore easy to see how the mode characteristics change as the feedback gain is increased from zero to a large value. Or, more generally, as $K_\theta \rightarrow \infty$ so

$$\begin{aligned} \omega_s &\rightarrow \infty \\ \zeta_s &\rightarrow 0 \end{aligned} \quad (11.27)$$

Similarly, with reference to equation (6.13), the characteristics of the phugoid mode are given approximately by

$$\begin{aligned} s^2 + \frac{(CD - BE)}{C^2}s + \frac{E}{C} &= s^2 + \left(\frac{8.728K_\theta^2 + 9.499K_\theta + 0.369}{21.716K_\theta^2 + 45.845K_\theta + 24.197} \right)s \\ &+ \left(\frac{0.103 + 0.167K_\theta}{4.919 + 4.66K_\theta} \right) = 0 \end{aligned} \quad (11.28)$$

Thus, again, as $K_\theta \rightarrow \infty$ so

$$\begin{aligned}\omega_p &\rightarrow \sqrt{\frac{0.167}{4.66}} = 0.184 \text{ rad/s} \\ 2\zeta_p\omega_p &\rightarrow \frac{8.728}{21.716} = 0.402 \text{ rad/s}\end{aligned}\tag{11.29}$$

and allowing for rounding errors,

$$\zeta_p \rightarrow 1.0\tag{11.30}$$

The conclusion is then, that negative pitch attitude feedback to elevator tends to destabilise the short period mode and increase its frequency whereas its effect on the phugoid mode is more beneficial. The phugoid stability is increased whilst its frequency also tends to increase a little but is bounded by an acceptable maximum value. For all practical purposes the frequency is assumed to be approximately constant. This result is, perhaps, not too surprising since pitch attitude is a dominant motion variable in phugoid dynamics and is less significant in short period pitching motion. It is quite clear that pitch attitude feedback to elevator is not the correct way to augment the longitudinal stability of the F-104.

What this approximate analysis does not show is the relative sensitivity of each mode to the feedback gain. This can only be evaluated by solving the characteristic equation repeatedly for a range of values of K_θ from zero to a suitably large value. A typical practical range of values might be $0 \leq K_\theta \leq 2 \text{ rad/rad}$, for example. This kind of analysis is most conveniently achieved with the aid of a *root locus plot*.

11.4 THE ROOT LOCUS PLOT

The *root locus plot* is a relatively simple tool for determining, by graphical means, detailed information about the stability of a closed loop system knowing only the open loop transfer function. The plot shows the roots, or *poles*, of the closed loop system characteristic equation for every value of a single loop variable, typically the feedback gain. It is therefore not necessary to calculate the roots of the closed loop characteristic equation for every single value of the chosen loop variable. As its name implies, the root locus plot shows loci on the s -plane of all the roots of the closed loop transfer function denominator as a function of the single loop gain variable.

The root locus plot was proposed by Evans (1954) and from its first appearance rapidly gained in importance as an essential control systems design tool. Consequently, it is described in most books concerned with linear control systems theory, for example it is described by Friedland (1987). Because of the relative mathematical complexity of the underlying theory, Evans (1954) main contribution was the development of an approximate asymptotic procedure for manually “sketching” closed loop root loci on the s -plane without recourse to extensive calculation. This was achieved with the aid of a set of “rules” which resulted in a plot of sufficient accuracy for most design purposes. It was therefore essential that control system designers were familiar with the rules. Today, the root locus plot is universally produced by computational means. It is no longer necessary for the designer to know the rules although

he must still know how to interpret the plot correctly and, of course, he must know its limitations.

In aeronautical applications it is vital to understand the correct interpretation of the root locus plot. This is especially so when it is being used to evaluate augmentation schemes for the precise control of the stability characteristics of an aircraft over the flight envelope. In the opinion of the author, this can only be done from the position of strength which comes with a secure knowledge of the rules for plotting a root locus by hand. For this reason the rules are set out in Appendix 11. However, it is not advocated that root locus plots should be drawn by hand, this is unnecessary when computational tools such as *MATLAB* and *Program CC* are readily available. The processes involved in the construction of a root locus plot are best illustrated by example as follows.

Example 11.2

Consider the use of the root locus plot to evaluate the effect of pitch attitude feedback to elevator on the F-104 aircraft at the same flight condition as discussed in Example 11.1. The closed loop system block diagram applying is that shown in Fig. 11.6. The open loop system transfer function is, from equation (11.20),

$$\frac{\theta(s)}{\eta(s)} = \frac{-4.66K_\theta(s + 0.133)(s + 0.269)}{(s^2 + 0.015s + 0.021)(s^2 + 0.911s + 4.884)} \text{ rad/rad} \quad (11.31)$$

with poles and zeros,

$$\begin{aligned} p_1 &= -0.0077 + 0.1448j \\ p_2 &= -0.0077 - 0.1448j \\ p_3 &= -0.4553 + 2.1626j \\ p_4 &= -0.4553 - 2.1626j \\ z_1 &= -0.133 \\ z_2 &= -0.269 \end{aligned} \quad \begin{array}{l} \text{whence} \\ \text{Number of poles } n_p = 4 \\ \text{Number of zeros } n_z = 2 \end{array}$$

The open loop poles and zeros are mapped on to the s -plane as shown in Fig. 11.7. The loci of the closed loop poles are then plotted as the feedback gain K_θ is allowed to increase from zero to a large value. In this example the loci were obtained computationally and are discussed in the context of the *rules* set out in Appendix 11.

Rule 1 locates the poles and zeros on the s -plane and determines that, since there are two more poles than zeros, four loci commence at the poles, two of which terminate at the zeros and two of which go off to infinity as $K_\theta \rightarrow \infty$.

Rule 2 determines that the real axis between the two zeros is part of a locus.

Rule 3 determines that the two loci which go off to infinity do so asymptotically to lines at 90° and at 270° to the real axis.

Rule 4 determines that the asymptotes radiate from the cg of the plot located at -0.262 on the real axis.

Rule 5 determines the point on the real axis at which two loci break-in to the locus between the two zeros. Method 1, the approximate method, determines the break-in

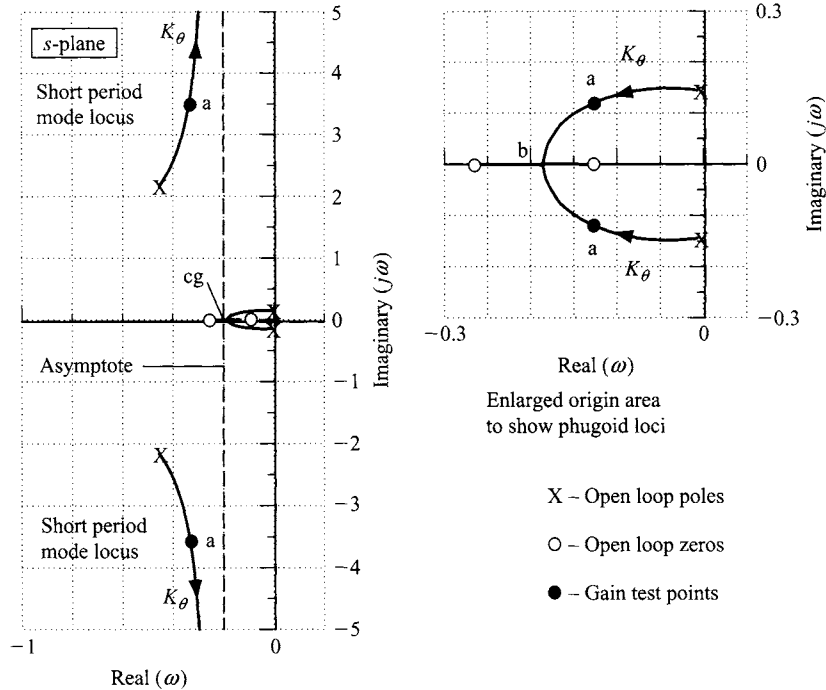


Figure 11.7 Example of root locus plot construction.

point at -0.2 . Method 2, the exact method, determines the break-in point at -0.186 . Either value is satisfactory for all practical purposes.

Rule 6 simply states that the two loci branching into the real axis do so at $\pm 90^\circ$ to the real axis.

Rule 7 determines the angle of departure of the loci from the poles and the angles of arrival at the zeros. This is rather more difficult to calculate by hand and to do so, the entire s -plane plot is required. The angles given by the computer program used to plot the loci are as follows:

- angle of departure from p_1 , 194°
- angle of departure from p_2 , -194°
- angle of departure from p_3 , 280°
- angle of departure from p_4 , -280°
- angle of arrival at z_1 , 180°
- angle of arrival at z_2 , 0°

Note that these values compare well with those calculated by hand from measurements made on the s -plane using a protractor.

Rule 8 enables the total loop gain to be evaluated at any point on the loci. To do this by hand is particularly tedious, it requires a plot showing the entire s -plane

and it is not always very accurate, especially if the plot is drawn to a small scale. However, since this is the primary reason for plotting root loci in the first instance all computer programs designed to plot root loci provide a means for obtaining values of the feedback gain at test points on the loci. Not all root locus plotting programs provide the information given by rules 4, 5 and 7. In this example the feedback gain at test point a is $K_\theta = -1.6$ and at test point b, the break-in point, $K_\theta = -12.2$. Note that, in this example, the feedback gain has units $^\circ/\circ$ or, equivalently rad/rad. When all test points of interest have been investigated the root locus plot is complete.

One of the more powerful features of the root locus plot is that it gives explicit information about the relative sensitivity of the stability modes to the feedback in question. In this example, the open loop aircraft stability characteristics are

$$\text{Phugoid damping ratio } \zeta_p = 0.0532$$

$$\text{Phugoid undamped natural frequency } \omega_p = 0.145 \text{ rad/s}$$

$$\text{Short period damping ratio } \zeta_s = 0.206$$

$$\text{Short period undamped natural frequency } \omega_s = 2.21 \text{ rad/s}$$

and at test point a, where $K_\theta = -1.6$, the closed loop stability characteristics are

$$\text{Phugoid damping ratio } \zeta_p = 0.72$$

$$\text{Phugoid undamped natural frequency } \omega_p = 0.17 \text{ rad/s}$$

$$\text{Short period damping ratio } \zeta_s = 0.10$$

$$\text{Short period undamped natural frequency } \omega_s = 3.49 \text{ rad/s}$$

Thus the phugoid damping is increased by about 14 times and its frequency remains nearly constant. In fact, the oscillatory phugoid frequency can never exceed 0.186 rad/s. The short period mode damping is approximately halved whilst its frequency is increased by about 50%. Obviously the phugoid damping is the parameter which is most sensitive to the feedback gain by a substantial margin. A modest feedback gain of say, $K_\theta = -0.1$ rad/rad would result in a very useful increase in phugoid damping whilst causing only very small changes in the other stability parameters. However, the fact remains that pitch attitude feedback to elevator destabilises the short period mode by reducing the damping ratio from its open loop value. This then, is not the cure for the poor short period mode stability exhibited by the open loop F-104 aircraft at this flight condition. All of these conclusions support the findings of Example 11.1 but, clearly, very much greater analytical detail is directly available from inspection of the root locus plot.

Additional important points relating to the application of the root locus plot to aircraft stability augmentation include the following:

- Since the plot is symmetric about the real axis it is not necessary to show the lower half of the s -plane, unless the plot is constructed by hand. All of the relevant information provided by the plot is available in the upper half of the s -plane.
- At typical scales it is frequently necessary to obtain a plot of the origin area at enlarged scale in order to resolve the essential detail. This is usually very easy to achieve with most computational tools.

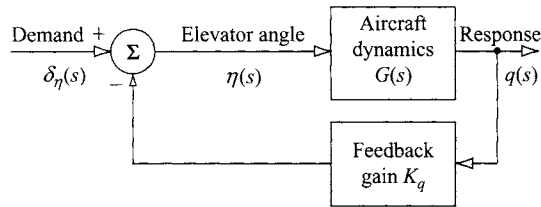


Figure 11.8 A simple pitch rate feedback system.

- As has been mentioned previously, it is essential to be aware of the sign of the open loop aircraft transfer function. Most root locus plotting computer programs assume the standard positive transfer function with negative feedback. A negative transfer function will result in an incorrect locus. The easy solution to this problem is to enter the transfer function with a positive sign and to change the sign of the feedback gains given by the program. However, it is important to remember the changes made when assessing the result of the investigation.

Example 11.3

In Examples 11.1 and 11.2 it is shown that pitch attitude feedback to elevator is not the most appropriate means for augmenting the deficient short period mode damping of the F-104. The correct solution is to augment pitch damping by implementing pitch rate feedback to elevator, velocity feedback in servo mechanism terms. The control system functional block diagram is shown in Fig. 11.8.

For the same flight condition, a take-off configuration, as in the previous examples, the pitch rate response to elevator transfer function for the Lockheed F-104 Starfighter was obtained from Teper (1969) and may be written in factorised form,

$$\frac{q(s)}{\eta(s)} = \frac{-4.66s(s + 0.133)(s + 0.269)}{(s^2 + 0.015s + 0.021)(s^2 + 0.911s + 4.884)} \text{ rad/s/rad} \quad (11.32)$$

As before, the stability modes of the open loop aircraft are,

$$\text{Phugoid damping ratio } \zeta_p = 0.0532$$

$$\text{Phugoid undamped natural frequency } \omega_p = 0.145 \text{ rad/s}$$

$$\text{Short period damping ratio } \zeta_s = 0.206$$

$$\text{Short period undamped natural frequency } \omega_s = 2.21 \text{ rad/s}$$

With reference to MIL-F-8785C (1980), defining the F-104 as a class IV aircraft, operating in flight phase category C and assuming Level 1 flying qualities are desired then, the following constraints on the stability modes may be determined:

$$\text{Phugoid damping ratio } \zeta_p \geq 0.04$$

$$\text{Short period damping ratio } \zeta_s \geq 0.5$$

$$\text{Short period undamped natural frequency } 0.8 \leq \omega_s \leq 3.0 \text{ rad/s}$$

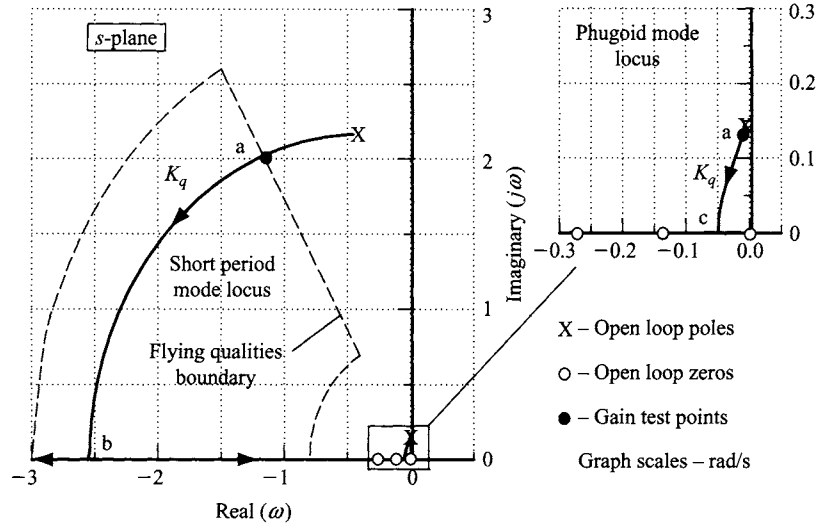


Figure 11.9 Root locus plot showing pitch rate feedback to elevator.

The upper limit on short period mode damping ratio is ignored since it is greater than one. Additionally, the closed loop phugoid frequency should ideally conform to $\omega_p \leq 0.1 \omega_s$ where, here ω_s is the closed loop short period mode frequency. Clearly, the unaugmented aircraft meets these flying qualities requirements with the exception of the short period mode damping ratio which is much too low.

The root locus plot constructed from the transfer function, equation (11.32), is shown in Fig. 11.9. Also shown on the same s -plane plot are the flying qualities short period mode boundaries according to the limits determined from MIL-F-8785C and quoted above.

Clearly, pitch rate feedback to elevator is ideal since it causes the damping of both the phugoid and short period modes to be increased although the short period mode is most sensitive to feedback gain. Further, the frequency of the short period mode remains more-or-less constant through the usable range of values of feedback gain K_q . For the same range of feedback gains the frequency of the phugoid mode is reduced thereby increasing the separation between the frequencies of the two modes. At test point a $K_q = -0.3$ rad/rad/s which is the smallest feedback gain required to bring the closed loop short period mode into agreement with the flying qualities boundaries. Allowing for a reasonable margin of error and uncertainty a practical choice of feedback gain might be $K_q = -0.5$ rad/rad/s. The stability augmentation control law would then be

$$\eta = \delta_\eta + 0.5q \quad (11.33)$$

This augmentation system is the classical *pitch damper* used on many aeroplanes from the same period as the Lockheed F-104 and typical feedback gains would be in the range $-0.1 \leq K_q \leq -1.0$ rad/rad/s. It is not known what value of feedback gain is used in the F-104 at this flight condition but the published description of the longitudinal augmentation system structure is the same as that shown in Fig. 11.8.

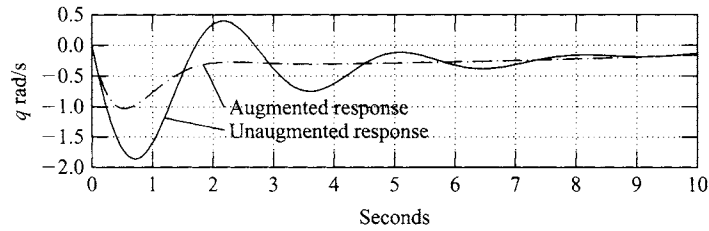


Figure 11.10 Pitch rate response to a unit elevator step input.

Substituting the control law, equation (11.33), into the open loop longitudinal equations of motion as described in Section 11.3 enables the closed loop equations of motion to be derived. Solution of the equations in the usual way gives the response transfer functions for the augmented aircraft. Solution of the closed loop characteristic equation determines that at $K_q = -0.5 \text{ rad/rad/s}$ the longitudinal modes have the following characteristics:

$$\text{Phugoid damping ratio } \zeta_p = 0.079$$

$$\text{Phugoid undamped natural frequency } \omega_p = 0.133 \text{ rad/s}$$

$$\text{Short period damping ratio } \zeta_s = 0.68$$

$$\text{Short period undamped natural frequency } \omega_s = 2.41 \text{ rad/s}$$

Clearly, at this value of feedback gain the flying qualities requirements are met completely with margins sufficient to allow for uncertainty. The closed loop system thus defined provides the basis for further analytical studies concerning the implementation architecture and safety issues. The pitch rate response of the aircraft before and after the addition of the augmentation loop is illustrated in Fig. 11.10. The first 10 s of the response to a unit elevator step input is shown to emphasise the considerable improvement in short period mode stability. The longer term response is not shown since this is not changed significantly by the augmentation and, in any event, the phugoid dynamics are acceptable.

11.5 LONGITUDINAL STABILITY AUGMENTATION

In Examples 11.2 and 11.3 it has been shown how negative feedback using a single variable can be used to selectively augment the stability characteristics of an aeroplane. It has also been shown how the effect of single variable feedback may readily be evaluated with the aid of a root locus plot. Now clearly, the choice of feedback variable is important in determining the nature of the change in the stability characteristics of the aeroplane since each variable results in a unique combination of changes. Provided that the aircraft is equipped with the appropriate motion sensors various feedback control schemes are possible and it then becomes necessary to choose the feedback variable(s) best suited to augment the deficiencies of the basic airframe. It is also useful to appreciate what effect each feedback variable has on the stability modes

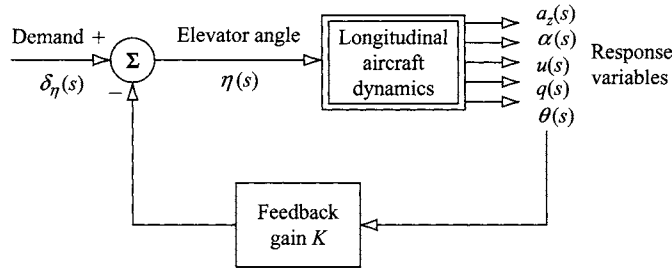


Figure 11.11 Longitudinal feedback options.

when assessing a FCS design. However complex the functional structure of the system the basic augmentation effect of each feedback variable does not change. Feedback is also used for reasons other than stability augmentation, for example, in autopilot functions. In such cases augmentation will also occur and it may not be desirable, in which case a thorough understanding of the effects of the most commonly used feedback variables is invaluable.

In order to evaluate the effect of feedback utilising a particular response variable it is instructive to conduct a survey of all the single loop feedback options. In every case the feedback loop is reduced to a simple gain component only. By this means the possible intrusive effects of other loop components, such as noise filters, phase compensation filters, sensor and actuator dynamics, are prevented from masking the true augmentation effects. The longitudinal stability augmentation options are summarised in Fig. 11.11 in which it is implied that a negative feedback loop may be closed between any of the motion variables and the elevator. Other loops could of course be closed between the motion variables and alternative longitudinal control motivators, or engine thrust control, for example, but these are not considered here.

The survey is conducted by taking each motion variable in turn and evaluating its influence on the closed loop stability characteristics as a function of the loop gain K . The root locus plot is an especially useful tool for this purpose since it enables the relative influence on, and the relative sensitivity of, each of the stability modes to be assessed simultaneously. As the detailed effect of feedback depends on the aircraft and flight condition of interest it is not easy to generalise and is best illustrated by example. Consequently the following survey, Example 11.4, is based on a typical aircraft operating at a typical flight condition and the observations may be applied loosely to the longitudinal stability augmentation of most aircraft.

Example 11.4

Transfer function data for the McDonnell Douglas A-4D Skyhawk aircraft was obtained from Teper (1969). The flight condition chosen corresponds with an all up weight of 17,578 lb at an altitude of 35,000 ft at Mach 0.6. In factorised form the longitudinal characteristic equation is

$$\Delta(s) = (s^2 + 0.014s + 0.0068)(s^2 + 1.009s + 5.56) = 0 \quad (11.34)$$

and the longitudinal stability mode characteristics are

$$\text{Phugoid damping ratio } \zeta_p = 0.086$$

$$\text{Phugoid undamped natural frequency } \omega_p = 0.082 \text{ rad/s}$$

$$\text{Short period damping ratio } \zeta_s = 0.214$$

$$\text{Short period undamped natural frequency } \omega_s = 2.358 \text{ rad/s}$$

These stability mode characteristics would normally be considered acceptable with the exception of the short period mode damping ratio which is too low. The Skyhawk is typical of combat aeroplanes of the 1960s in which modest degrees of augmentation only are required to rectify the stability deficiencies of the basic airframe. This, in turn, implies that modest feedback gains only are required in the range say, typically, $0 \leq K \leq 2.0$. In modern FBW aircraft having unstable airframes rather larger gain values would be required to achieve the same levels of augmentation. In general, the greater the required change in the stability characteristics the greater the feedback gains needed to effect the change. In the following catalogue of root locus plots each plot illustrates the effect of a single feedback loop closure as a function of increasing feedback gain K .

(i) *Pitch attitude feedback to elevator*

The open loop aircraft transfer function is

$$\frac{\theta(s)}{\eta(s)} \equiv \frac{N_\eta^\theta(s)}{\Delta(s)} = \frac{-8.096(s - 0.0006)(s + 0.3591)}{(s^2 + 0.014s + 0.0068)(s^2 + 1.009s + 5.56)} \text{ rad/rad} \quad (11.35)$$

and the corresponding root locus plot is shown in Fig. 11.12.

As K_θ is increased the phugoid damping increases rapidly whilst the frequency remains nearly constant. Whereas, as K_θ is increased the short period mode frequency increases whilst the damping decreases, both characteristics changing relatively slowly. Thus, as might be expected since pitch attitude is a dominant variable in the phugoid mode, this mode is considerably more sensitive to the loop gain than the short period mode. Since this feedback option further destabilises the short period mode its usefulness in a SAS is very limited indeed. However, it does improve phugoid stability, the mode becoming critically damped at a gain of $K_\theta = -0.37 \text{ rad/rad}$. A practical gain value might be $K_\theta = -0.1 \text{ rad/rad}$ which would result in a good level of closed loop phugoid stability without reducing the short period mode stability too much. These observations are, of course, in good agreement with the findings of Example 11.2.

(ii) *Pitch rate feedback to elevator*

The open loop aircraft transfer function is

$$\frac{q(s)}{\eta(s)} \equiv \frac{N_\eta^q(s)}{\Delta(s)} = \frac{-8.096s(s - 0.0006)(s + 0.3591)}{(s^2 + 0.014s + 0.0068)(s^2 + 1.009s + 5.56)} \text{ rad/s/rad} \quad (11.36)$$

and the corresponding root locus plot is shown in Fig. 11.13.

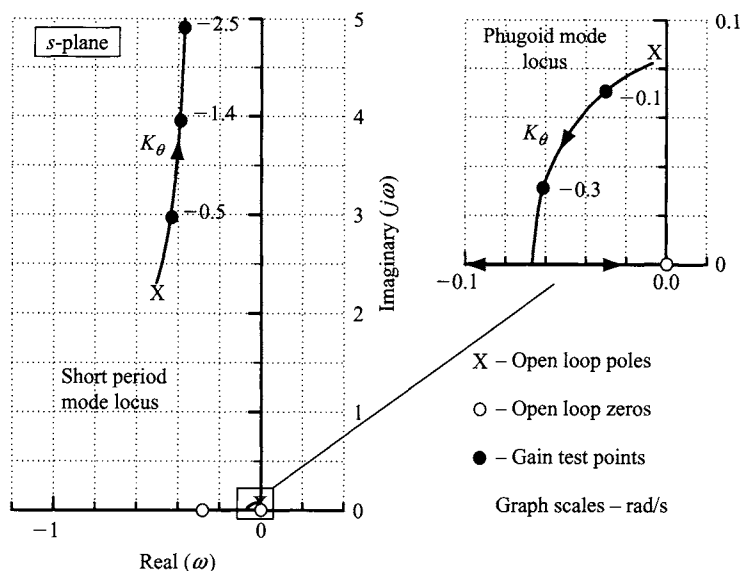


Figure 11.12 Root locus plot – pitch attitude feedback to elevator.

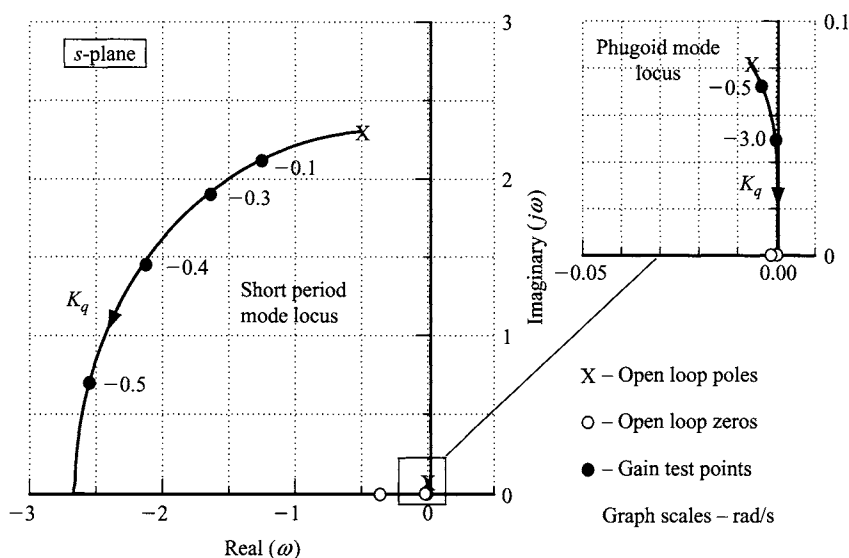


Figure 11.13 Root locus plot – pitch rate feedback to elevator.

As K_q is increased the short period mode damping increases rapidly whilst the frequency remains nearly constant. Whereas, as K_q is increased the phugoid frequency and damping decrease relatively slowly. More typically, a slow increase in phugoid damping would be seen. Thus, as might be expected since pitch rate is a dominant variable in the short period mode, this mode is considerably

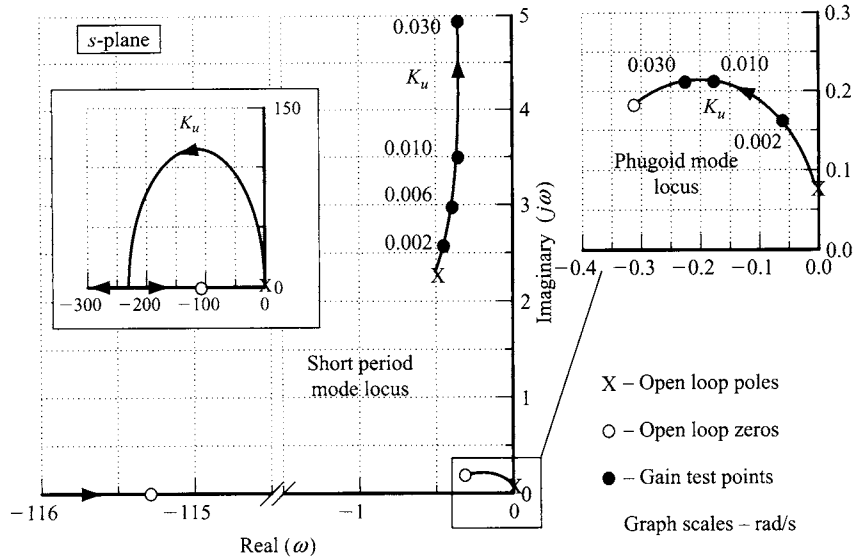


Figure 11.14 Root locus plot – velocity feedback to elevator.

more sensitive to the loop gain than the phugoid mode. As discussed in Example 11.3 this feedback option describes the classical pitch damper and is found on many aeroplanes. It also exactly describes the longitudinal stability augmentation solution used on the Skyhawk. Its dominant effect is to artificially increase the magnitude of the derivative m_q , it also increases the magnitude of the derivatives x_q and z_q but to a lesser degree. The short period mode becomes critically damped at a gain of $K_q = -0.53$ rad/rad/s. A practical gain value might be $K_q = -0.3$ rad/rad/s which would result in an adequate level of closed loop short period mode stability whilst simultaneously increasing the frequency separation between the two modes. However, at this value of feedback gain the changes in the phugoid characteristics would be almost insignificant. As before, these observations are in good agreement with the findings of Example 11.3.

(iii) *Velocity feedback to elevator*

The open loop aircraft transfer function is

$$\frac{u(s)}{\eta(s)} \equiv \frac{N_\eta^u(s)}{\Delta(s)} = \frac{6.293(s^2 + 0.615s + 0.129)(s + 115.28)}{(s^2 + 0.014s + 0.0068)(s^2 + 1.009s + 5.56)} \text{ ft/s/rad} \quad (11.37)$$

and the corresponding root locus plot is shown in Fig. 11.14.

As K_u is increased the short period mode frequency increases quite rapidly whilst, initially, the damping decreases. However, at very large gain values the damping commences to increase again to eventually become critical. Whereas, as K_u is increased both the frequency and damping of the phugoid mode increase relatively rapidly. Thus, at this flight condition both modes appear to have similar sensitivity to feedback gain. The stabilising influence on the phugoid mode

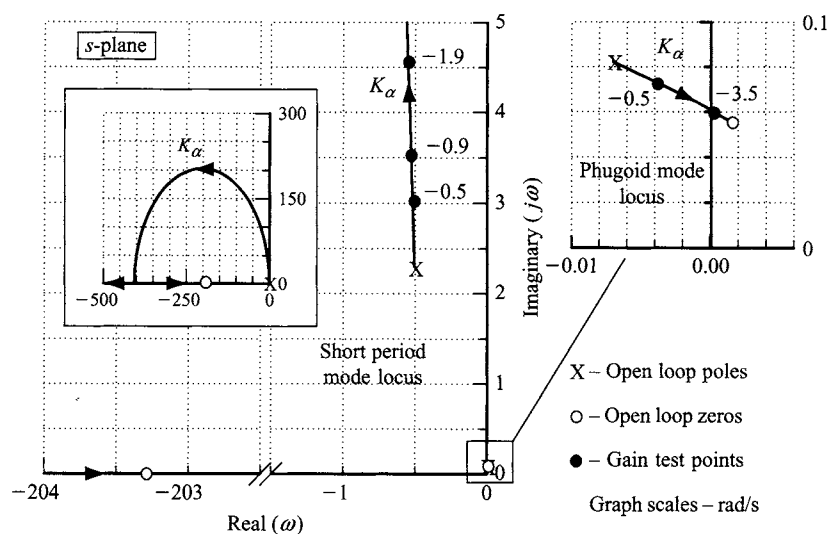


Figure 11.15 Root locus plot – incidence feedback to elevator.

is much as might be expected since velocity is the dominant variable in the mode dynamics. The dominant effect of the feedback is therefore to artificially increase the magnitude of the derivative m_u and since m_u is usually small it is not surprising that even modest values of feedback gain have a significant effect on phugoid stability. It also increases the magnitude of the derivatives x_u and z_u but to a lesser degree. A practical gain value might be $K_u = 0.001$ rad/ft/s which would result in a significant improvement in closed loop phugoid mode stability whilst simultaneously decreasing the stability of the short period mode by a small amount. However, such values of feedback gain are quite impractically small and in any event this feedback option would not find much useful application in a conventional longitudinal SAS.

(iv) *Incidence angle feedback to elevator*

The open loop aircraft transfer function is

$$\frac{\alpha(s)}{\eta(s)} \equiv \frac{N_\eta^\alpha(s)}{\Delta(s)} = \frac{-0.04(s^2 - 0.0027s + 0.0031)(s + 203.34)}{(s^2 + 0.014s + 0.0068)(s^2 + 1.009s + 5.56)} \text{ rad/rad} \quad (11.38)$$

and the corresponding root locus plot is shown in Fig. 11.15.

As K_α is increased the short period mode frequency increases very rapidly whilst, initially, the damping decreases slowly. However, as the gain increases further the damping slowly starts to increase to eventually become critical at an impractically large value of feedback gain. At all practical gain values the damping remains more-or-less constant. As K_α is increased both the frequency and damping of the phugoid are reduced, the mode becoming unstable at a gain of $K_\alpha = -3.5$ rad/rad in this example. Incidence feedback to elevator is a powerful method for augmenting the longitudinal static stability of an aeroplane and

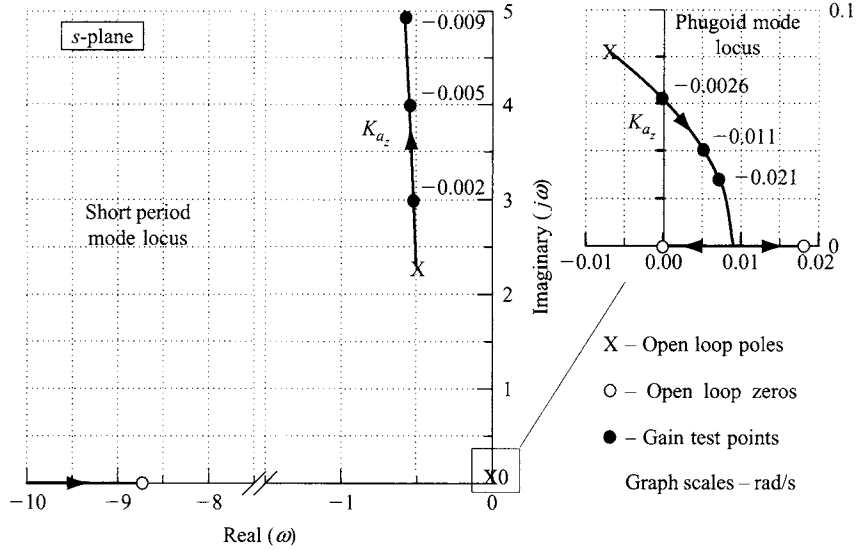


Figure 11.16 Root locus plot – normal acceleration feedback to elevator.

finds extensive application in unstable FBW aircraft. The effect of the feedback is equivalent to increasing the pitch stiffness of the aircraft which artificially increases the magnitude of the derivative m_w ($\partial C_m / \partial \alpha$) and to a lesser degree it also increases the magnitude of the derivatives x_w and z_w . Thus the increase in short period mode frequency together with the less significant influence on damping is entirely consistent with the augmentation option. Since phugoid dynamics are typically very nearly incidence constant, the expected effect of the feedback on the mode is negligible. This is not the case in this example, probably due to aerodynamic effects at the relatively high subsonic Mach number. This is confirmed by the fact that the phugoid roots do not even approximately cancel with the complex pair of numerator roots, which might normally be expected. It would therefore be expected to see some incidence variation in the phugoid dynamics.

(v) *Normal acceleration feedback to elevator*

The open loop aircraft transfer function is

$$\begin{aligned} \frac{a_z(s)}{\eta(s)} &\equiv \frac{N_\eta^{a_z(s)}}{\Delta(s)} \\ &= \frac{-23.037(s - 0.018)(s - 0.0003)(s + 8.717)(s - 8.203)}{(s^2 + 0.014s + 0.0068)(s^2 + 1.009s + 5.56)} \text{ ft/s}^2/\text{rad} \end{aligned} \quad (11.39)$$

and the corresponding root locus plot is shown in Fig. 11.16. Since the transfer function is *not proper* care must be exercised in the production of the root locus plot and in its interpretation. However, at typically small values of feedback gain its interpretation seems quite straightforward.

Since an accelerometer is rather more robust than an incidence sensor, normal acceleration feedback to elevator is commonly used instead of, or to complement, incidence feedback. Both feedback variables have a similar effect on the phugoid and short period stability mode at practical values of feedback gain. However, both modes are rather more sensitive to feedback gain since very small values result in significant changes to the mode characteristics. As K_{a_z} is increased the short period mode frequency increases very rapidly whilst, initially, the damping decreases slowly. However, as the gain increases further the damping slowly starts to increase to eventually become critical at an impractically large value of feedback gain. At all practical gain values the damping remains more-or-less constant. The full short period mode branch of the locus is not shown in Fig. 11.16 since the gain range required exceeded the capability of the computational software used to produce the plots. As K_{a_z} is increased both the frequency and damping of the phugoid are reduced, the mode becoming unstable at a gain of $K_{a_z} = 0.0026 \text{ rad/ft/sec}^2$ in this example. Since the normal acceleration variable comprises a mix of incidence, velocity and pitch rate (see Section 5.5) then the augmentation it provides in a feedback control system may be regarded as equivalent to the sum of the effects of feedback of the separate variables. Thus at moderate gains the increase in pitch stiffness is significant and results in a rapid increase in short period mode frequency. The corresponding increase in short period mode damping is rather greater than that achieved with incidence feedback alone due to the effect of implicit pitch rate feedback. Since the incidence dependent term dominates the determination of normal acceleration it is not surprising that normal acceleration feedback behaves like incidence feedback. It is approximately equivalent to artificially increasing the magnitude of the derivative m_w and to a lesser degree it also increases the magnitude of the derivatives x_w and z_w .

11.6 LATERAL-DIRECTIONAL STABILITY AUGMENTATION

As for the longitudinal stability augmentation options described in Section 11.5, it is also instructive to conduct a survey of all the lateral-directional single loop feedback options. The lateral-directional stability augmentation options are summarised in Fig. 11.17 in which it is implied that a negative feedback loop may be closed between any of the motion variables and either the ailerons or rudder. Other loops could be closed between the motion variables and alternative lateral-directional control motivators but, again, these are not considered here.

As before, the survey is conducted by taking each motion variable in turn and evaluating its influence on the closed loop stability characteristics as a function of the loop gain K . The detailed effects of the lateral-directional feedback options are much more dependent on the aircraft and flight condition than the longitudinal feedback options. Therefore, it is more difficult, and probably less appropriate, to generalise and the effects are also best illustrated by example. The following survey, Example 11.5, is based on a typical aircraft operating at a typical flight condition and the observations may be interpreted as being applicable to the lateral-directional stability augmentation of most aircraft. However, care must be exercised when applying the observations to other aircraft and every new application should be evaluated in its own right.

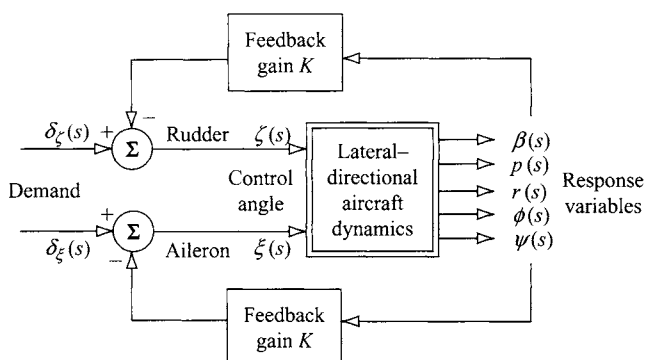


Figure 11.17 Lateral-directional feedback options.

Example 11.5

Transfer function data for the Northrop T-38 Talon aircraft was also obtained from Teper (1969). The flight condition chosen corresponds with an all up weight of 10,000 lb at Mach 0.8 at sea level. In factorised form the lateral-directional characteristic equation is

$$\Delta(s) = (s - 0.0014)(s + 4.145)(s^2 + 1.649s + 38.44) = 0 \quad (11.40)$$

and the lateral-directional stability mode characteristics are

$$\text{Spiral mode time constant } T_s = -714 \text{ s}$$

$$\text{Roll mode time constant } T_r = 0.24 \text{ s}$$

$$\text{Dutch roll damping ratio } \zeta_d = 0.133$$

$$\text{Dutch roll undamped natural frequency } \omega_d = 6.2 \text{ rad/s}$$

Clearly, the spiral mode is unstable, which is quite typical, and the time constant is sufficiently large that it is most unlikely to give rise to handling problems. In fact, all of the stability characteristics are better than the minimum acceptable for Level 1 flying qualities. However, the aircraft is fitted with a simple yaw damper to improve the lateral-directional flying and handling qualities at all flight conditions, including some where the minimum standards are not met. In the following catalogue of root locus plots each plot illustrates the effect of a single feedback loop closure as a function of increasing feedback gain K . It should be noted that in the original data source the sign convention for aileron angle is opposite to that adopted in this book. In the following illustrations the aileron sign convention is changed to be consistent with the British notation.

(i) Sideslip angle feedback to aileron

The open loop transfer function is

$$\frac{\beta(s)}{\xi(s)} \equiv \frac{N_\xi^\beta(s)}{\Delta(s)} = \frac{1.3235(s - 0.0832)(s + 7.43)}{(s - 0.0014)(s + 4.145)(s^2 + 1.649s + 38.44)} \text{ rad/rad} \quad (11.41)$$

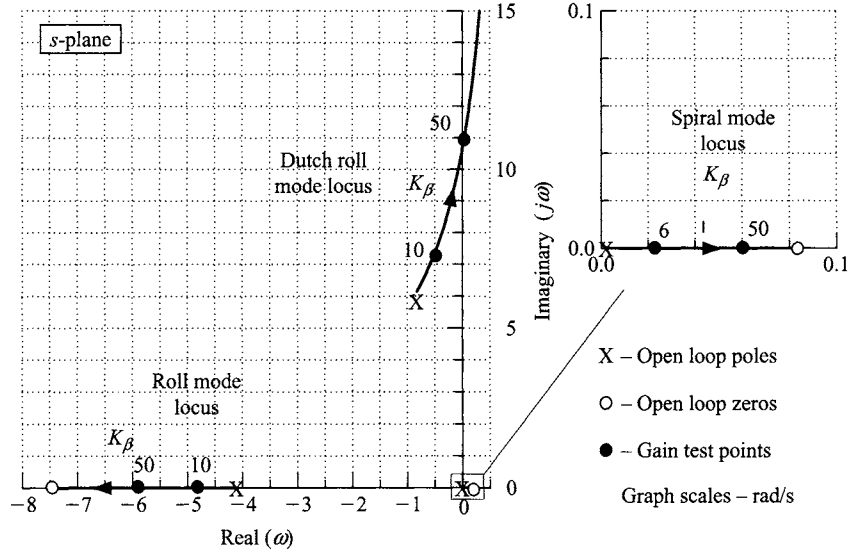


Figure 11.18 Root locus plot – sideslip angle feedback to aileron.

and the corresponding root locus plot is shown in Fig. 11.18.

As K_β is increased so the spiral mode pole moves further to the right on the s -plane and its instability is worsened as its time constant is reduced. The roll mode stability is increased as the gain K_β is increased since its pole moves to the left on the s -plane. As K_β is increased the dutch roll frequency is increased whilst its damping is decreased and it eventually becomes unstable at a gain of approximately $K_\beta = 50$ rad/rad. All three modes are relatively insensitive to the feedback since large gains are required to achieve modest changes in the mode characteristics although the spiral mode is the most sensitive. Negative feedback of sideslip angle to aileron is equivalent to an increase in dihedral effect. In particular, for this example, it augments the magnitude of the stability derivatives l_v and n_v and the degree of augmentation of each derivative depends on the value of K_β and the aileron control derivatives l_ξ and n_ξ respectively. Clearly, the effect is to artificially increase the lateral stiffness of the aeroplane resulting in an increase in dutch roll frequency and a corresponding increase in roll damping. It is unlikely that sideslip angle feedback to aileron alone would find much use in a SAS.

(ii) *Roll rate feedback to aileron*

The open loop transfer function is

$$\frac{p(s)}{\xi(s)} \equiv \frac{N_\xi^p(s)}{\Delta(s)} = \frac{-27.75(s - 0.0005)(s^2 + 1.55s + 41.91)}{(s - 0.0014)(s + 4.145)(s^2 + 1.649s + 38.44)} \text{ rad/s/rad} \quad (11.42)$$

and the corresponding root locus plot is shown in Fig. 11.19. Note that both the spiral mode pole and the dutch roll poles are approximately cancelled

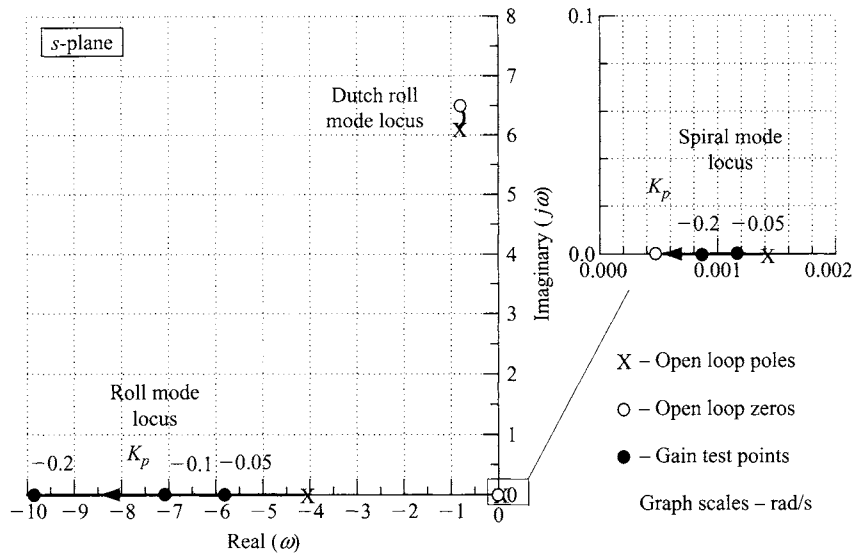


Figure 11.19 Root locus plot – roll rate feedback to aileron.

by the numerator zeros. This means that both modes are insensitive to this feedback option.

As K_p is increased so the spiral mode pole moves to the left on the s -plane and its instability is reduced as its time constant is increased. However, the spiral mode remains unstable at all values of K_p although roll rate feedback to aileron generally improves the handling qualities associated with the spiral mode. The roll mode stability increases rapidly as the gain K_p is increased since its pole moves to the left on the s -plane. The roll mode is most sensitive to this feedback option and, in fact, roll rate feedback to aileron describes the classical roll damper and is used in many aeroplanes. Whatever the value of K_p the effect on the stability characteristics of the dutch roll mode is insignificant as stated above. At all levels of feedback gain the dutch roll mode poles remain in a very small localised area on the s -plane. Negative roll rate feedback to aileron is equivalent to an increase in the roll damping properties of the wing. In particular it augments the magnitude of the stability derivative l_p and, to a lesser extent, n_p . As before, the degree of augmentation of each derivative depends on the value of K_p and the aileron control derivatives l_ξ and n_ξ respectively.

(iii) *Yaw rate feedback to aileron*

The open loop transfer function is

$$\frac{r(s)}{\xi(s)} \equiv \frac{N_\xi^r(s)}{\Delta(s)} = \frac{-1.712(s + 5.405)(s^2 + 1.788s + 4.465)}{(s - 0.0014)(s + 4.145)(s^2 + 1.649s + 38.44)} \text{ rad/s/rad} \quad (11.43)$$

and the corresponding root locus plot is shown in Fig. 11.20.

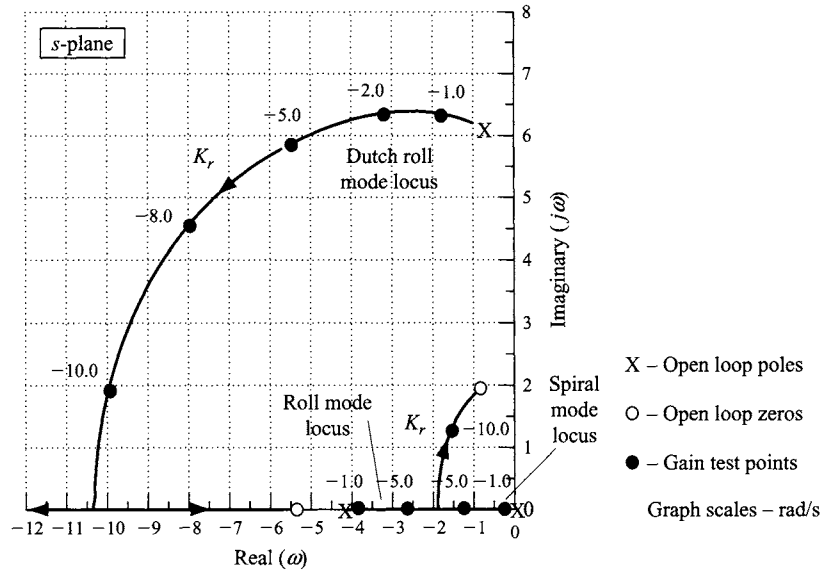


Figure 11.20 Root locus plot – yaw rate feedback to aileron.

As K_r is increased so the spiral mode pole moves to the left on the s -plane to become stable at a small value of gain. At a gain of approximately $K_r = 6.0$ rad/rad/s, which is somewhat greater than a practical value, the spiral and roll modes couple to form a stable low frequency oscillatory characteristic. The roll mode stability decreases as the gain K_r is increased since its pole moves to the right on the s -plane before coupling with the spiral mode. The dutch roll mode is the most sensitive mode and as K_r is increased the damping increases rapidly whilst the frequency increases rather more slowly. At practical levels of feedback gain the most useful improvements would be to stabilise the spiral mode and to improve dutch roll damping whilst degrading roll mode stability only slightly. However, yaw rate feedback to aileron cross couples both the roll and yaw control axes of the aeroplane and is not so desirable for safety reasons. The feedback is equivalent to an increase in the yaw damping properties of the wing. In particular it augments the magnitude of the stability derivatives l_r and n_r .

(iv) *Roll attitude feedback to aileron*

The open loop transfer function is

$$\frac{\phi(s)}{\xi(s)} \equiv \frac{N_\xi(s)}{\Delta(s)} = \frac{-27.75(s^2 + 1.55s + 41.91)}{(s - 0.0014)(s + 4.145)(s^2 + 1.649s + 38.44)} \text{ rad/rad} \quad (11.44)$$

and the corresponding root locus plot is shown in Fig. 11.21. Note that the dutch roll poles are approximately cancelled by the numerator zeros which implies that the mode is insensitive to this feedback option.

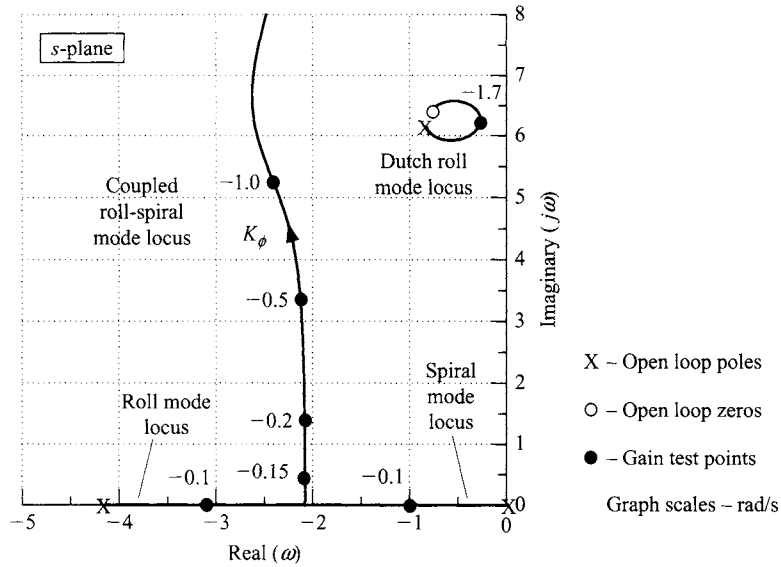


Figure 11.21 Root locus plot – roll attitude feedback to aileron.

As K_ϕ is increased the spiral mode pole moves to the left on the s -plane and its stability increases very rapidly, a very small value of gain being sufficient to place the pole on the left half of the s -plane. At a slightly larger value of gain, $K_\phi = -0.14$ rad/rad, the spiral and roll modes couple to form a low frequency oscillatory characteristic as in the previous illustration. Therefore, roll mode stability decreases rapidly as the gain K_ϕ is increased until its pole couples with that of the spiral mode. Clearly, both the roll and spiral modes are most sensitive to this feedback option. As expected, for all values of K_ϕ the effect on the stability characteristics of the dutch roll mode is insignificant. At all levels of feedback gain the dutch roll mode poles remain in a very small localised area on the s -plane and the minimum damping corresponds with a feedback gain of $K_\phi = -1.7$ rad/rad. Negative roll attitude feedback to aileron is, very approximately, equivalent to an increase in roll stiffness and at quite small feedback gain values manifests itself as the coupled roll–spiral oscillatory mode which may be regarded as a kind of lateral pendulum mode.

(v) *Yaw attitude feedback to aileron*

The open loop transfer function is

$$\frac{\psi(s)}{\xi(s)} \equiv \frac{N_\xi^\psi(s)}{\Delta(s)} = \frac{-1.712(s + 5.405)(s^2 + 1.788s + 4.465)}{s(s - 0.0014)(s + 4.145)(s^2 + 1.649s + 38.44)} \text{ rad/rad} \quad (11.45)$$

and the corresponding root locus plot is shown in Fig. 11.22.

As K_ψ is increased the spiral mode pole moves to the left on the s -plane, towards the pole at the origin, to which it couples at a very small value of gain

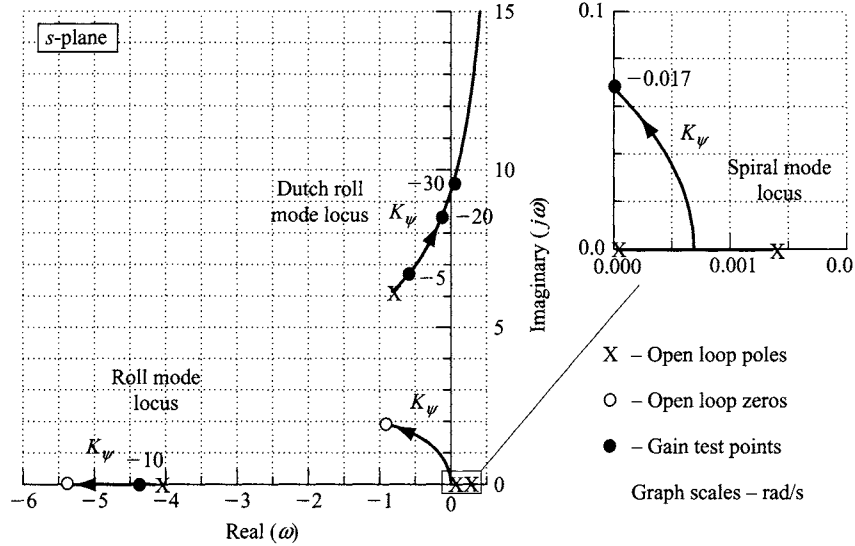


Figure 11.22 Root locus plot – yaw attitude feedback to aileron.

indeed to form a low frequency unstable oscillatory characteristic. At a gain of approximately $K_\psi = -0.017$ rad/rad the low frequency oscillatory characteristic becomes stable. The roll mode stability increases very slowly as the gain K_ψ is increased since its pole moves to the left on the s -plane towards the zero at -5.404 . As K_ψ is increased the dutch roll mode frequency increases whilst the damping decreases, both characteristics changing rather slowly. The dutch roll mode eventually becomes unstable at a gain of approximately $K_\psi = -30.0$ rad/rad. At practical levels of feedback gain the effect on the roll and dutch roll modes is almost insignificant. On the other hand the effect of the feedback on the spiral mode is most significant, even at very low values of gain. As in (iii), yaw attitude feedback to aileron cross couples both the roll and yaw control axes of the aeroplane and is not so desirable for safety reasons. The feedback is equivalent to an increase in the yaw stiffness properties of the wing.

(vi) *Sideslip angle feedback to rudder*

The open loop transfer function is

$$\frac{\beta(s)}{\zeta(s)} \equiv \frac{N_\zeta^\beta(s)}{\Delta(s)} = \frac{0.10(s - 0.0015)(s + 4.07)(s + 113.4)}{(s - 0.0014)(s + 4.145)(s^2 + 1.649s + 38.44)} \text{ rad/rad} \quad (11.46)$$

and the corresponding root locus plot is shown in Fig. 11.23. Note that both the spiral and roll mode poles are very nearly cancelled by numerator zeros. It may therefore be expected that negative sideslip angle feedback to rudder will only significantly augment the dutch roll mode.

As expected, as K_β is increased both the spiral mode pole and the roll mode pole move to the right on the s -plane but the reduction in stability

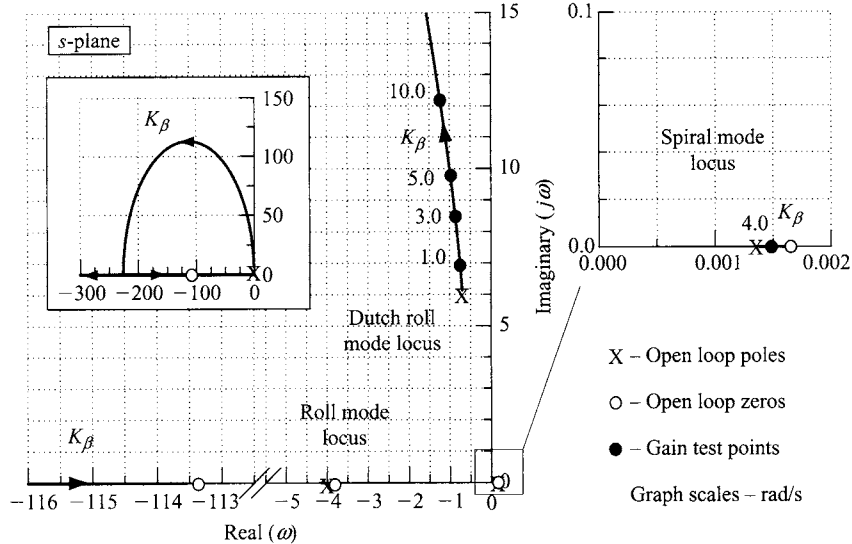


Figure 11.23 Root locus plot – sideslip angle feedback to rudder.

really is insignificant. As K_β is increased both the dutch roll frequency and damping are increased, the mode eventually becoming critically damped at the absurdly high frequency of $\omega_d = 226$ rad/s at a gain of approximately $K_\beta = 4500$ rad/rad! Negative feedback of sideslip angle to rudder is equivalent to an increase in the weathercock effect of the fin, or yaw stiffness. In particular, for this example, it very effectively augments the magnitude of the stability derivative n_v and to lesser extent l_v . The degree of augmentation of each derivative depends on the value of K_β and the rudder control derivatives n_ζ and l_ζ respectively. Clearly, the effect is to artificially increase the directional stiffness of the aeroplane resulting in an increase in dutch roll frequency and a corresponding, but much slower, increase in roll damping. At all practical values of feedback gain the dutch roll damping remains more-or-less constant at its open loop value.

(vii) *Roll rate feedback to rudder*

The open loop transfer function is

$$\frac{p(s)}{\zeta(s)} \equiv \frac{N_\zeta^p(s)}{\Delta(s)} = \frac{16.65(s - 0.0006)(s - 0.79)(s + 1.09)}{(s - 0.0014)(s + 4.145)(s^2 + 1.649s + 38.44)} \text{ rad/s/rad} \quad (11.47)$$

and the corresponding root locus plot is shown in Fig. 11.24. Note that the spiral mode pole is very approximately cancelled by a numerator zero. It is therefore expected that the spiral mode will be insensitive to this feedback option.

As expected the effect on the spiral mode of this feedback option is insignificant. The roll mode stability increases rapidly as the gain K_p is increased since its pole moves to the left on the s -plane. The roll mode is quite sensitive to this feedback option, which is not surprising since roll rate is the dominant

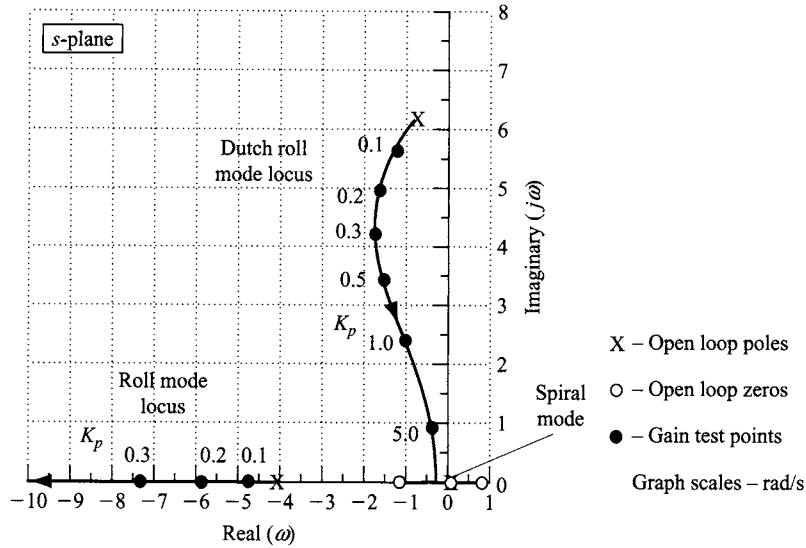


Figure 11.24 Root locus plot – roll rate feedback to rudder.

motion variable in the aircraft dynamics associated with the mode. The dutch roll mode is also very sensitive to this feedback option. As K_p is increased the dutch roll damping increases rapidly whilst the frequency is reduced. For values of the feedback gain $K_p \geq 8.9$ rad/rad/s the dutch roll mode is critically damped and is therefore non-oscillatory. Negative roll rate feedback to rudder is equivalent to an increase in the yaw damping properties of the wing. In particular it augments the magnitude of the stability derivative n_p and, to a lesser extent, l_p . As before, the degree of augmentation of each derivative depends on the value of K_p and the rudder control derivatives n_ζ and l_ζ respectively.

(viii) *Yaw rate feedback to rudder*

The open loop transfer function is

$$\frac{r(s)}{\zeta(s)} \equiv \frac{N_\zeta'(s)}{\Delta(s)} = \frac{-11.01(s + 0.302)(s + 0.366)(s + 4.11)}{(s - 0.0014)(s + 4.145)(s^2 + 1.649s + 38.44)} \text{ rad/s/rad} \quad (11.48)$$

and the corresponding root locus plot is shown in Fig. 11.25. Note that the roll mode pole is almost exactly cancelled by a numerator zero. It is therefore expected that the roll mode will be insensitive to this feedback option.

The spiral mode stability increases rapidly as the gain K_r is increased since its pole moves to the left on the s -plane. The spiral mode is very sensitive to this feedback option and becomes stable at a gain of $K_r = -0.4$ rad/rad/s. As expected the effect of this feedback option on the roll mode is insignificant. The branching of the loci around the roll mode simply indicates that the pole-zero cancellation is not exact. The dutch roll mode is also very sensitive to this feedback option. As K_r is increased the dutch roll damping

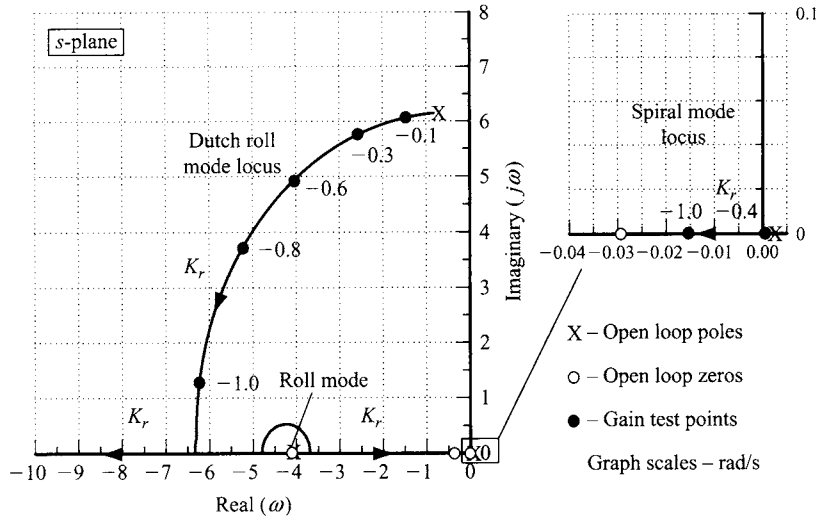


Figure 11.25 Root locus plot – yaw rate feedback to rudder.

increases rapidly whilst the frequency remains almost constant. For values of the feedback gain $K_r \leq -1.2$ rad/rad/s the dutch roll mode becomes critically damped. Practical values of feedback gain would, typically, be in the range $0 \geq K_r \geq -0.7$ rad/rad/s. The dutch roll mode damping is most sensitive to this feedback option and yaw rate feedback to rudder describes the classical yaw damper, which is probably the most common augmentation system. However, its use brings a bonus since it also improves the spiral mode stability significantly. Negative yaw rate feedback to rudder is equivalent to an increase in the yaw damping properties of the aeroplane or, to an increase in the effectiveness of the fin as a damper. In particular it augments the magnitude of the stability derivative n_r and, to a lesser extent, l_r .

(ix) *Roll attitude feedback to rudder*

The open loop transfer function is

$$\frac{\phi(s)}{\zeta(s)} \equiv \frac{N_\zeta^\phi(s)}{\Delta(s)} = \frac{16.5(s - 0.825)(s + 1.08)}{(s - 0.0014)(s + 4.145)(s^2 + 1.649s + 38.44)} \text{ rad/rad} \quad (11.49)$$

and the corresponding root locus plot is shown in Fig. 11.26.

As K_ϕ is increased the spiral mode pole moves to the right on the s -plane and its stability decreases slowly. The roll mode stability also decreases slowly as the gain K_ϕ is increased, a gain of $K_\phi \cong 4.0$ rad/rad being required to double the time constant, for example. As K_ϕ is increased the dutch roll mode frequency increases relatively quickly. The damping ratio also increases a little initially but, as the gain is increased further the damping decreases steadily to zero at infinite feedback gain. Negative roll attitude feedback to rudder is, very approximately, equivalent to an increase in directional stiffness

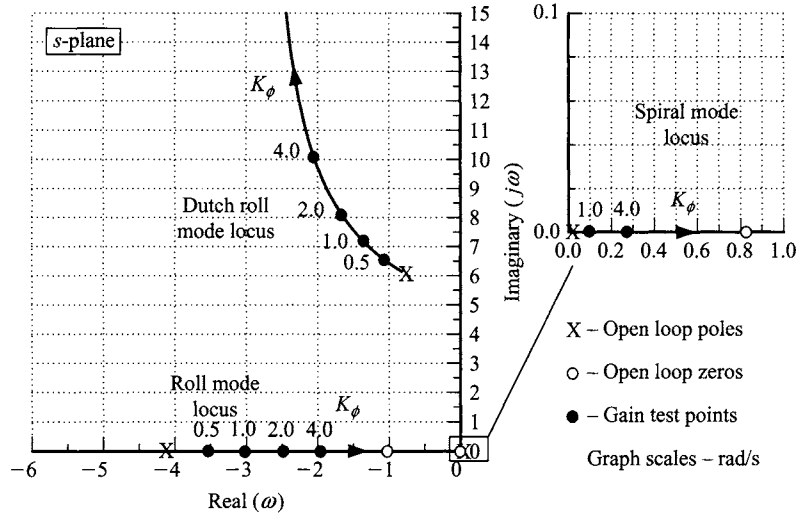


Figure 11.26 Root locus plot – roll attitude feedback to rudder.

and is not commonly used in autostabilisation systems since it introduces cross-coupling between the roll and yaw control axes.

(x) *Yaw attitude feedback to rudder*

The open loop transfer function is

$$\frac{\psi(s)}{\zeta(s)} \equiv \frac{N_{\zeta}^{\psi}(s)}{\Delta(s)} = \frac{-11.01(s + 0.0302)(s + 0.367)(s + 4.11)}{s(s - 0.0014)(s + 4.145)(s^2 + 1.649s + 38.44)} \text{ rad/rad} \quad (11.50)$$

and the corresponding root locus plot is shown in Fig. 11.27. Note that the roll mode pole is almost exactly cancelled by a numerator zero indicating that the mode is not sensitive to this feedback option.

As K_{ψ} is increased the spiral mode pole moves to the left on the s -plane, towards the pole at the origin, to which it couples at a very small value of gain to form a stable low frequency oscillatory characteristic at all practical small values of gain. At a gain of approximately $K_{\psi} = -1.5$ rad/rad the low frequency oscillatory characteristic becomes critically damped. Since the frequency of this mode is so low, and when stable it is reasonably well damped, it is unlikely to give rise to handling problems. As expected the roll mode stability remains effectively unchanged by this feedback option. As K_{ψ} is increased the dutch roll mode frequency increases whilst the damping decreases, both characteristics changing relatively slowly. The dutch roll mode eventually becomes neutrally stable at infinite feedback gain. At practical levels of feedback gain the effect on the dutch roll mode is to increase the frequency with only a very small reduction in damping. Negative yaw attitude feedback to rudder is equivalent to an increase in directional stiffness and is not commonly used in autostabilisation systems.

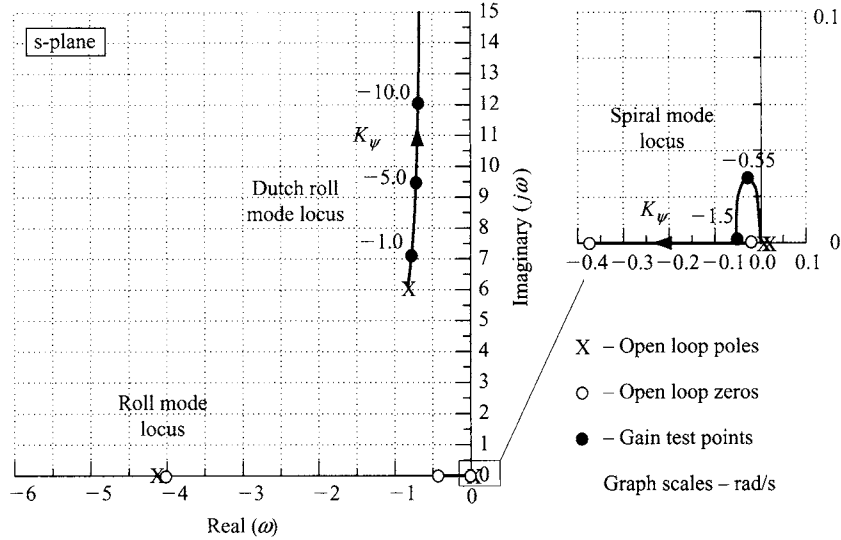


Figure 11.27 Root locus plot – yaw attitude feedback to rudder.

11.7 THE POLE PLACEMENT METHOD

An alternative and very powerful method for designing feedback gains for autostabilisation systems is the *pole placement method*. The method is based on the manipulation of the equations of motion in state space form and makes full use of the appropriate computational tools in the analytical process. Practical application of the method to aeroplanes is limited since it assumes that all state, or motion, variables are available for use in an augmentation system, which is not usually the case. However, regardless of the limitations of the method, it can be very useful to the FCS designer in the initial stages of assessment of augmentation system structure.

The state and output matrix equations describing the unaugmented, or open loop, aircraft, equations (5.48), are written

$$\begin{aligned}\dot{\mathbf{x}}(t) &= \mathbf{A}\mathbf{x}(t) + \mathbf{B}\mathbf{u}(t) \\ \mathbf{y}(t) &= \mathbf{C}\mathbf{x}(t) + \mathbf{D}\mathbf{u}(t)\end{aligned}\quad (11.51)$$

Assuming that augmentation is achieved by negative feedback of the state vector $\mathbf{x}(t)$ to the input vector $\mathbf{u}(t)$ then the control law may be written

$$\mathbf{u}(t) = \mathbf{v}(t) - \mathbf{K}\mathbf{x}(t) \quad (11.52)$$

where, $\mathbf{v}(t)$ is a vector of input demand variables and \mathbf{K} is a matrix of feedback gains. Note that equation (11.52) is the general multi-variable equivalent of equation (11.14). The closed loop state and output equations describing the augmented aircraft are obtained by substituting equation (11.52) into equations (11.51)

$$\begin{aligned}\dot{\mathbf{x}}(t) &= [\mathbf{A} - \mathbf{BK}]\mathbf{x}(t) + \mathbf{B}\mathbf{v}(t) \\ \mathbf{y}(t) &= [\mathbf{C} - \mathbf{DK}]\mathbf{x}(t) + \mathbf{D}\mathbf{v}(t)\end{aligned}\quad (11.53)$$

or, more simply,

$$\begin{aligned}\dot{\mathbf{x}}(t) &= \mathbf{A}_{aug}\mathbf{x}(t) + \mathbf{B}\mathbf{v}(t) \\ \mathbf{y}(t) &= \mathbf{C}_{aug}\mathbf{x}(t) + \mathbf{D}\mathbf{v}(t)\end{aligned}\quad (11.54)$$

Equations (11.54) are solved in exactly the same way as those of the open loop aircraft, equations (11.51), to obtain the response transfer functions for the augmented aircraft. Note that (as discussed in Section 5.6) for typical aircraft applications the direct matrix $\mathbf{D} = 0$, the output matrix $\mathbf{C} = \mathbf{I}$, the identity matrix, and equations (11.51) to (11.54) simplify accordingly.

Now the characteristic equation of the augmented aircraft is given by

$$\Delta_{aug}(s) = |s\mathbf{I} - \mathbf{A}_{aug}| \equiv |s\mathbf{I} - \mathbf{A} + \mathbf{BK}| = 0 \quad (11.55)$$

and the roots of equation (11.55), or equivalently the eigenvalues of \mathbf{A}_{aug} , describe the stability characteristics of the augmented aircraft.

Subject to the constraint that the open loop state equations (11.51) describes a *controllable system*, which an aircraft is, then a feedback matrix \mathbf{K} exists such that the eigenvalues of the closed loop system may be completely specified. Thus if the required stability and control characteristics of the augmented aircraft are specified, the roots of equation (11.55) may be calculated and knowing the open loop state and input matrices, \mathbf{A} and \mathbf{B} , respectively, then equation (11.55) may be solved to find \mathbf{K} . Thus this method enables the stability characteristics of the augmented aircraft to be designed completely and exactly as required. Equivalently, this therefore means that the poles of the closed loop aircraft may be *placed* on the s -plane exactly as required. However, full state feedback is essential if all of the closed loop poles are to be placed on the s -plane as required.

When the controlled system is *single input* then the feedback matrix \mathbf{K} is unique and only one set of feedback gains will provide the required stability characteristics. When the controlled system is *multi-input* then an infinite number of gain matrices \mathbf{K} may be found which will provide the required stability characteristics. Consequently, most control system design problems involving the use of the pole placement method are solved by arranging the open loop system as a single input system. This is most easily done when dealing with aircraft stability augmentation since the inputs naturally separate into elevator, ailerons, rudder and thrust at the most basic level. It is a simple matter to arrange the state equation to include only one input variable and then to apply the pole placement method to design an augmentation system feedback structure.

Example 11.6

The longitudinal equations of motion for the McDonnell Douglas F-4C Phantom aircraft were obtained from Heffley and Jewell (1972). At the chosen flight condition the weight is 38,925 lb and the aircraft is flying at Mach 1.1 at sea level. The state equations (11.51) were derived for the unaugmented aircraft from the data provided to give,

$$\mathbf{A} = \begin{bmatrix} -0.068 & -0.011 & 0 & -9.81 \\ 0.023 & -2.10 & 375 & 0 \\ 0.011 & -0.160 & -2.20 & 0 \\ 0 & 0 & 1 & 0 \end{bmatrix} \quad \mathbf{B} = \begin{bmatrix} -0.41 & 1.00 \\ -77.0 & -0.09 \\ -61.0 & -0.11 \\ 0 & 0 \end{bmatrix}$$

with state vector, $\mathbf{x}^T = [u \ w \ q \ \theta]$ and input vector, $\mathbf{u}^T = [\eta \ \tau]$. Note that two input variables are given in the model, elevator angle η and thrust τ . Using *Program CC* the equations of motion were solved and the open loop characteristic polynomial was found,

$$\Delta(s) = (s^2 + 4.3s + 64.6)(s^2 + 0.07s + 0.003) \quad (11.56)$$

and the corresponding longitudinal stability mode characteristics are

$$\text{Phugoid damping ratio } \zeta_p = 0.646$$

$$\text{Phugoid undamped natural frequency } \omega_p = 0.054 \text{ rad/s}$$

$$\text{Short period damping ratio } \zeta_s = 0.267$$

$$\text{Short period undamped natural frequency } \omega_s = 8.038 \text{ rad/s}$$

Referring to the flying qualities requirements in MIL-F-8785C (1980) it was found that for a class IV aeroplane in the most demanding category A flight phase the Phantom comfortably meets Level 1 requirements with the exception of short period mode damping, which is too low. Clearly, some augmentation is required to improve the pitch damping in particular.

The design decision was made to increase the short period mode damping ratio to 0.7 whilst retaining the remaining stability characteristics at the nominal values of the basic unaugmented airframe. A short period mode damping ratio of 0.7 was chosen since this gives a good margin of stability and results in the shortest mode settling time after a disturbance. However, the exact value chosen is not important provided that the margin of stability is adequate to allow for uncertainty in the modelling. Therefore, the pole placement method is to be used to give the augmented aircraft the following longitudinal stability characteristics

$$\text{Phugoid damping ratio } \zeta_p = 0.65$$

$$\text{Phugoid undamped natural frequency } \omega_p = 0.054 \text{ rad/s}$$

$$\text{Short period damping ratio } \zeta_s = 0.7$$

$$\text{Short period undamped natural frequency } \omega_s = 8.0 \text{ rad/s}$$

Thus the required closed loop characteristic polynomial is

$$\Delta_{aug}(s) = (s^2 + 11.2s + 64.0)(s^2 + 0.07s + 0.003) \quad (11.57)$$

Since a single input control system is required, the input being elevator angle, the open loop state equation is modified accordingly, simply by removing the thrust terms. The open loop state equation may then be written,

$$\begin{bmatrix} \dot{u} \\ \dot{w} \\ \dot{q} \\ \dot{\theta} \end{bmatrix} = \begin{bmatrix} -0.068 & -0.011 & 0 & -9.81 \\ 0.023 & -2.10 & 375 & 0 \\ 0.011 & -0.160 & -2.20 & 0 \\ 0 & 0 & 1 & 0 \end{bmatrix} \begin{bmatrix} u \\ w \\ q \\ \theta \end{bmatrix} + \begin{bmatrix} -0.41 \\ -77.0 \\ -61.0 \\ 0 \end{bmatrix} \eta \quad (11.58)$$

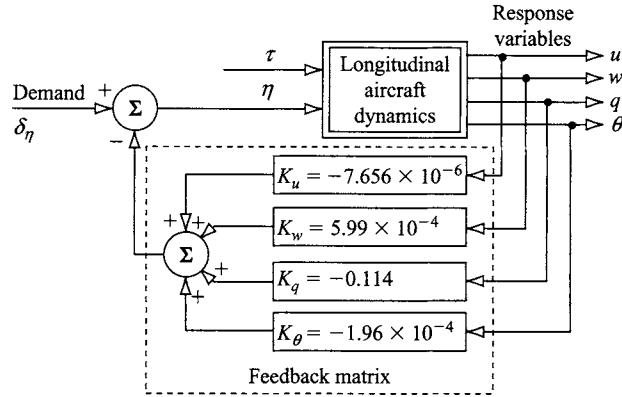


Figure 11.28 Longitudinal full state feedback to elevator.

With the aid of the pole placement tool in *Program CC* the feedback gain matrix required to give the augmented aircraft the characteristic polynomial (equation (11.57)) was determined,

$$\begin{aligned}\mathbf{K} &= [K_u \quad K_w \quad K_q \quad K_\theta] \\ &= [-7.7 \times 10^{-6} \quad 5.99 \times 10^{-4} \quad -0.114 \quad -1.96 \times 10^{-4}]\end{aligned}\quad (11.59)$$

Care is required in order to maintain the correct units of the elements in the feedback matrix. The SAS control law is obtained by substituting for \mathbf{K} in equation (11.52) whence,

$$\eta = \delta_\eta - K_u u - K_w w - K_q q - K_\theta \theta \quad (11.60)$$

The corresponding closed loop control system structure follows and is shown in Fig. 11.28.

Now clearly, the choice of closed loop stability characteristics has resulted in a gain matrix in which the gains K_u , K_w and K_θ are impractically and insignificantly small. This is simply due to the fact that the only significant change between the open and closed loop stability characteristics is the increase in short period mode damping and, as has already been established in Examples 11.3 and 11.4, the pole placement method confirms that this can be achieved with pitch rate feedback to elevator alone. If additional changes in the stability characteristics were required then the gains K_u , K_w and K_θ would, of course, not necessarily be insignificant. Let the feedback gain matrix be simplified to include only practical gain values and equation (11.59) may be written,

$$\mathbf{K} = [0 \quad 0 \quad -0.12 \quad 0] \quad (11.61)$$

The closed loop state equation (11.53), may then be calculated by writing,

$$\mathbf{K} = \begin{bmatrix} 0 & 0 & -0.12 & 0 \\ 0 & 0 & 0 & 0 \end{bmatrix} \quad (11.62)$$

where the second row describes the feedback to the second, thrust, input, which is not used in this example for the reason given above. $[\mathbf{A} - \mathbf{BK}]$ is easily calculated with the aid of *Program CC* for example and the closed loop state equation, written to include both input variables, is

$$\begin{bmatrix} \dot{u} \\ \dot{w} \\ \dot{q} \\ \dot{\theta} \end{bmatrix} = \begin{bmatrix} -0.068 & -0.011 & -0.049 & -9.81 \\ 0.023 & -2.10 & 366 & 0 \\ 0.011 & -0.160 & -9.52 & 0 \\ 0 & 0 & 1 & 0 \end{bmatrix} \begin{bmatrix} u \\ w \\ q \\ \theta \end{bmatrix} + \begin{bmatrix} -0.41 & 1.00 \\ -77.0 & -0.09 \\ -61.0 & -0.11 \\ 0 & 0 \end{bmatrix} \begin{bmatrix} \eta \\ \tau \end{bmatrix} \quad (11.63)$$

Comparison of the open loop equation (11.58) and the closed loop equation (11.63) indicates, as expected, that the only changes occur in the third column of the state matrix, the column associated with the variable q . The augmented state equation (11.63) is readily solved to obtain the closed loop transfer function matrix,

$$\begin{bmatrix} u(s) \\ w(s) \\ q(s) \\ \theta(s) \end{bmatrix} = \mathbf{G}(s) \begin{bmatrix} \eta(s) \\ \tau(s) \end{bmatrix} = \frac{\mathbf{N}(s)}{\Delta_{aug}(s)} \begin{bmatrix} \eta(s) \\ \tau(s) \end{bmatrix} \quad (11.64)$$

where the numerator matrix is given by

$$\mathbf{N}(s) = \begin{bmatrix} -0.41(s + 1.36)(s - 44.45)(s + 45.31) & 1.0(s + 0.027)(s^2 + 11.60s + 79.75) \\ -77.0(s - 0.003)(s + 0.071)(s + 299.3) & -0.09(s + 0.008)(s - 0.044)(s + 456.4) \\ -61.0s(s + 0.068)(s + 1.90) & -0.11s(s - 0.022)(s + 1.96) \\ -61.0(s + 0.068)(s + 1.90) & -0.11(s - 0.022)(s + 1.96) \end{bmatrix} \quad (11.65)$$

and the closed loop characteristic polynomial is

$$\Delta_{aug}(s) = (s^2 + 11.62s + 78.49)(s^2 + 0.07s + 0.002) \quad (11.66)$$

The corresponding longitudinal stability mode characteristics are

$$\text{Phugoid damping ratio } \zeta_p = 0.71$$

$$\text{Phugoid undamped natural frequency } \omega_p = 0.049 \text{ rad/s}$$

$$\text{Short period damping ratio } \zeta_s = 0.656$$

$$\text{Short period undamped natural frequency } \omega_s = 8.86 \text{ rad/s}$$

Thus by simplifying the feedback gain matrix to an approximate equivalent it is not surprising that the specified stability characteristics (defined by equation (11.57)) have also only been achieved approximately. However, the differences are small and

are quite acceptable. The main objective, to increase the short period mode damping to a reasonable level has been achieved comfortably. The changes in the stability characteristics caused by the feedback are in complete agreement with the observations made in Examples 11.3 and 11.4.

Note that the numerators of the closed loop transfer functions describing response to elevator, given in the first column of the numerator matrix in equation (11.65), are unchanged by the feedback which is also in accordance with earlier findings concerning the effect of feedback. However, the numerators of the closed loop transfer functions describing response to thrust, given in the second column of the numerator matrix in equation (11.65), include some changes. The numerators $N_r^u(s)$ and $N_r^w(s)$ are both changed a little by the effect of feedback whereas, the numerators $N_r^q(s)$ and $N_r^\theta(s)$ remain unchanged.

It will be noted that the longitudinal stability augmentation for the F-4A could just as easily have been “designed” with the aid of a single input–single output root locus plot as described in Example 11.3. However, the subsequent calculation of the closed loop response transfer functions would have been rather more laborious. The pole placement method is undoubtedly a very powerful design tool, especially for the preliminary assessment of the feedback gains needed to achieve a specified level of closed loop stability. Once the gains required to achieve a given set of augmented stability characteristics have been determined their values will not be significantly changed by subsequent increases in FCS complexity. The main disadvantage of the method, especially in aircraft applications, is that it assumes all motion variables are sensed and are available for use in a control system. This is not often the case. Then it is necessary to simplify the feedback structure, making use of the understanding provided by Examples 11.4 and 11.5, to achieve a reasonable performance compromise – much as illustrated by this example. It is also good practice to minimise the demands on the augmentation system by limiting the required changes to the stability characteristics. Remember that small changes result in small feedback gains, again, much as illustrated by this example.

REFERENCES

- Anon. 1980: *Military Specification – Flying Qualities of Piloted Airplanes*. MIL-F-8785C. Department of Defense, USA.
- Evans, W.R. 1954: *Control-System Dynamics*. McGraw-Hill Book Company, Inc., New York.
- Friedland, B. 1987: *Control System Design*. McGraw-Hill Book Company, New York.
- Heffley, R.K. and Jewell, W.F. 1972: *Aircraft Handling Qualities Data*. NASA Contractor Report, NASA CR-2144, National Aeronautics and Space Administration, Washington D.C. 20546.
- Teper, G.L. 1969: *Aircraft Stability and Control Data*. Systems Technology, Inc., STI Technical Report 176-1. NASA Contractor Report, National Aeronautics and Space Administration, Washington D.C. 20546.

PROBLEMS

1. Discuss and illustrate why, in a simple SAS is it sometimes necessary to vary the feedback gain with flight condition. (CU 1986)

2. The damping of the longitudinal short period mode may be augmented with pitch rate feedback to elevator. Write the reduced order longitudinal equations of motion in matrix form to include the feedback term. It may be assumed that the derivative Z_q is negligibly small. From the closed loop equations of motion obtain an expression for the characteristic equation. Hence, show that when the derivative $M_{\dot{w}}$ is assumed to be negligibly small, the value of feedback gain K_q required to double the damping ratio of the short period mode is given by

$$K_q = - \left(\frac{I_y}{m} \frac{\dot{Z}_w}{\dot{M}_\eta} + \frac{\dot{M}_q}{\dot{M}_\eta} \right)$$

Using the following aerodynamic data for the Republic F-105 Thunderchief aircraft, calculate a value of K_q and comment on the practicality of using such a value. (CU 1986)

Flight condition			Dimensionless derivatives			
Altitude	h	35,000 ft	X_u	-0.0599	M_u	0
Flight path angle	γ	0°	X_w	0.0714	M_w	-0.8021
Body incidence	α_e	0°	X_q	0	$M_{\dot{w}}$	-0.8718
Airspeed	V_0	270 m/s	X_η	0	M_q	-4.1303
Mass	m	18,680 kg	Z_u	-0.1427	M_η	-1.365
Pitch inertia	I_y	189,812 kgm ²	Z_w	-4.1188		
Air density	ρ	0.3798 kg/m ³	Z_q	0		
Wing area	S	36.45 m ²	Z_η	-0.7672		
mac	\bar{c}	3.54 m				

3. The open loop yaw rate response to rudder transfer function for the Republic F-105 Thunderchief aircraft flying at Mach 0.9 at an altitude of 35,000 ft is given by

$$\frac{r(s)}{\zeta(s)} = \frac{-4.71(s + 1.848)(s^2 + 0.053s + 0.067)}{(s - 0.0087)(s + 2.13)(s^2 + 1.211s + 10.82)} 1/s$$

Draw a root locus plot to show the effect of yaw rate feedback to rudder with feedback gain K_r .

- With the aid of the root locus plot, explain how it may be used to evaluate the effect of feedback on the characteristics modes of motion.
 - How does yaw rate feedback to rudder improve lateral-directional flying qualities?
 - What value of gain K_r is required to increase the dutch roll mode damping ratio to 0.25? For this value of K_r obtain values for the roots of the closed loop characteristic equation and compare the characteristics of the three modes with those of the unaugmented aircraft. (CU 1986)
4. Assuming the lateral response to aileron control comprises pure rolling motion only, derive the reduced order roll rate response to aileron control transfer

function for an aircraft. When the lateral stability of the aircraft is augmented by feeding back roll rate to aileron via the gain K_p , show that the augmented roll damping derivative is given by

$$\dot{L}_{p_{aug}} = \dot{L}_p - K_p \dot{L}_\xi$$

where, \dot{L}_p is the rolling moment due to roll rate and \dot{L}_ξ is the rolling moment due to aileron for the unaugmented aircraft.

Using the simple lateral model, assess the roll subsidence mode of the Northrop T-38 Talon aircraft. Data for the aircraft are tabulated below. What is the minimum value of K_p for which the aircraft will meet the flying qualities requirements?

Flight condition			Dimensionless derivatives			
Altitude	h	25,000 ft	Y_v	-1.260	N_v	0.240
Flight path angle	γ	0°	Y_p	0	N_p	0.0430
Body incidence	α_e	0°	Y_r	0	N_r	-0.170
Airspeed	V_0	123.7 m/s	Y_ξ	0	N_ξ	0.007
Mass	m	4540 kg	Y_ζ	0.160	N_ζ	-0.103
Roll inertia	I_x	5965 kgm ²				
Yaw inertia	I_z	46097 kgm ²	L_v	-0.097		
Inertia product	I_{xz}	0 kgm ²	L_p	-0.110		
Air density	ρ	0.549 kg/m ³	L_r	0.078		
Wing area	S	15.79 m ²	L_ξ	0.040		
Wing span	b	7.69 m	L_ζ	0.017		

(CU 1987)

5. Longitudinal flight condition and aerodynamic derivative data are given in the following table for a canard configured FBW combat aircraft.

Flight condition			Dimensionless derivatives			
Altitude	h	Sea level	X_u	0.050	M_u	0.003
Flight path angle	γ	0°	X_w	0.260	M_w	0.280
Body incidence	α_e	0°	X_q	0	$M_{\dot{w}}$	0.380
Airspeed	V_0	100 m/s	X_η	0	M_q	-0.500
Mass	m	12,500 kg	Z_u	-1.200	M_η	0.160
Pitch inertia	I_y	105,592 kgm ²	Z_w	-2.800		
Air density	ρ	1.225 kg/m ³	$Z_{\dot{w}}$	-0.700		
Wing area	S	50.0 m ²	Z_q	-1.200		
mac	\bar{c}	5.7 m	Z_η	-0.040		

- (i) Write down the reduced order longitudinal equations of motion appropriate to the aircraft. Hence, show that the short period mode characteristic equation is given approximately in terms of concise derivatives by

$$s^2 - (z_w + m_q + m_{\dot{w}}U_e)s - (m_wU_e - z_wm_q) = 0$$

State all assumptions made.

- (ii) Since the aircraft is unstable it is augmented with a control law of form,

$$\eta = \delta_\eta - K_q q - K_\alpha \alpha$$

What values of the feedback gains K_q and K_α are required to produce an augmented short period mode with natural frequency 5 rad/s and damping ratio 0.5? (CU 1989)

6. Explain why the dutch roll mode characteristics are often unacceptable in large civil transport aircraft.

The yaw control transfer function for a large civil transport aircraft cruising at 33,000 ft is given by

$$\frac{N_\zeta^r(s)}{\Delta(s)} = \frac{-1.17(s + 1.28)(s^2 - 0.04s + 0.10)}{(s + 0.004)(s + 1.25)(s^2 + 0.20s + 2.25)} 1/s$$

Evaluate the stability modes characteristics and assess these for Level 1 flying qualities.

The aircraft is fitted with a yaw damper to improve the dutch roll characteristics. Draw a root locus plot showing the effect of yaw rate feedback to rudder via gain K_r . Draw mode limit boundaries on the root locus plot corresponding with Level 1 flying qualities and suggest a suitable value for K_r . Evaluate all three modes for the chosen value of feedback gain and comment on the comparison with those of the unaugmented aircraft. (CU 1989)

7. Explain why the stability characteristics of the short term stability modes are critical to good flying qualities. Explain and illustrate how they may be augmented when those of the basic airframe are inadequate. (CU 2001)